ELSEVIER

Experimental Hematology

Experimental Hematology 2011;39:351–359

Functional characterization of hematopoietic stem cells in the spleen

Yohei Morita[a,*], Akiko Iseki[a,*], Satoshi Okamura[a], Sachie Suzuki[a], Hiromitsu Nakauchi[a], and Hideo Ema[b]

[a]*Division of Stem Cell Therapy;* [b]*Laboratory of Developmental Stem Cell Biology, Center for Stem Cell Biology and Regenerative Medicine, Institute of Medical Science, University of Tokyo, Tokyo, Japan*

(Received 7 July 2010; revised 13 December 2010; accepted 17 December 2010)

Objective. **Hematopoietic stem cells (HSCs) reside in both bone marrow (BM) and spleen in adult mice. However, whether BM and spleen HSCs are functionally similar is not known. Spleen HSCs were compared with BM HSCs by various assays.**

Materials and Methods. **Whole BM and spleen cells were quantitatively analyzed by competitive repopulation. Single-cell transplantation was performed with HSCs purified from BM and spleen. A parabiosis model was used to distinguish organ-specific HSCs from circulating HSCs. The cell cycle was analyzed with pyronin Y staining and bromodeoxyuridine uptake.**

Results. **Repopulating and self-renewal potentials were similar on a clonal basis between BM and spleen HSCs, whereas the HSC frequency in the spleen was significantly lower than that in the BM. Analysis of parabiotic mice suggested that most HSCs are long-term residents in each organ. Cell-cycle analysis revealed that spleen HSCs cycle twice as frequently as do BM HSCs, suggesting that G_0 phase length is longer in BM HSCs than in spleen HSCs. The cycling difference between BM and spleen HSCs was also observed in mice that had been reconstituted with BM or spleen cells, suggesting that HSC quiescence is regulated in an organ-specific manner.**

Conclusions. **Spleen HSCs and BM HSCs are functionally similar, but their cycling behaviors differ.** **© 2011 ISEH - Society for Hematology and Stem Cells. Published by Elsevier Inc.**

The spleen is a hematopoietic organ in adult mice. During embryonic development, hematopoietic stem cells (HSCs) migrate from the liver and possibly also from the placenta into the spleen around embryonic day 14 as well as into the bone marrow (BM) around embryonic day 17 [1–4]. Thereafter, HSCs reside in both spleen and BM throughout the life of a mouse. The spleen serves as an active hematopoietic organ in lethally irradiated mice for a while after transplantation with BM cells. The spleen is a major site of extramedullary hematopoiesis in pathological conditions, such as myeloproliferative diseases.

Microenvironments or niches are considered to play an important role in the regulation of HSCs [5]. Endosteal and perivascular regions have been proposed for niche sites in the BM [6], and osteoblasts and vascular endothelial cells are considered to be the major components in endosteal and perivascular niches, respectively [7–10]. Other types of cells might be involved in organization of the BM niches [11–14]. Because there are no osteoblasts in the spleen, regulation of HSCs in the spleen may differ from those in the BM. Apart from niches' cellular components, we hypothesized that these two organs contain functionally distinct niches. To gain insight into the niche as a functional entity in stem cell regulation, we compared the functional and behavioral differences between BM and spleen HSCs.

Materials and methods

Mice

C57BL/6 mice congenic for the Ly5 locus (B6-Ly5.1 mice) were bred and maintained at Sankyo Labo Service (Tsukuba, Japan). B6-Ly5.2 mice were purchased from Japan SLC (Hamamatsu, Japan). All procedures were approved by the Animal Care and Use Committee, Institute of Medical Science, University of Tokyo.

*Drs. Morita and Iseki contributed equally to this work.

Offprint requests to: Hideo Ema, M.D., Laboratory of Developmental Stem Cell Biology, Center for Stem Cell and Regenerative Medicine, Institute of Medical Science, University of Tokyo, 4-6-1 Shirokanedai, Minato-ku, Tokyo 108-8639, Japan; E-mail: hema@ims.u-tokyo.ac.jp

Supplementary data associated with this article can be found in the online version at doi:10.1016/j.exphem.2010.12.008.

0301-472X/$ - see front matter. Copyright © 2011 ISEH - Society for Hematology and Stem Cells. Published by Elsevier Inc.
doi: 10.1016/j.exphem.2010.12.008

Competitive repopulation

Femora, tibiae, and spleen were dissected from 8- to 12-week-old male B6-Ly5.1 mice. Bones were crushed using a mortar and pestle. Spleens were smashed between two glass slides. Cells were suspended in phosphate-buffered saline (PBS). A mixture of 1×10^6 BM or spleen cells (Ly5.1) and 1×10^6 BM cells from B6-Ly5.2 mice was transplanted into each of 10 B6-Ly5.2 mice irradiated at a dose of 9.5 Gy. Peripheral blood cells from the recipient mice were analyzed 4, 8, 12, and 16 weeks after transplantation. After erythrocyte lysis, cells were stained with biotinylated anti-Ly5.1, fluorescein isothiocyanate–conjugated anti-Ly5.2, phycoerythrin-cyanin 7 (PE-Cy7)–conjugated anti-B220, PE-conjugated anti-CD4 and -CD8, and allophycocyanin (APC)-conjugated anti–Mac-1 and –Gr-1 antibodies. The biotinylated antibody was developed with streptavidin-Alexa 594. Cells were analyzed using a FACS Vantage SE flow cytometer equipped with argon (488 nm) and dye (599 nm) lasers (BD Bioscience, San Jose, CA, USA). Percent chimerism was defined as (percent $Ly5.1^+$ test donor cells) (100)/(percent $Ly5.1^+$ test donor cells + percent $Ly5.2^+$ competitor cells). Repopulating unit (RU) values were calculated as (percent chimerism) (number of competitor cells)/(100 − percent chimerism) (10^5) [15].

For in vivo limiting-dilution assays [16], graded numbers of BM or spleen cells from three B6-Ly5.1 mice were mixed with 2×10^5 BM cells from B6-Ly5.2 mice and were transplanted into 10 or more lethally irradiated B6-Ly5.2 mice. When the percentage of chimerism comprising all myeloid, B-lymphoid, and T-lymphoid lineages was 1.0 or more 12 weeks after transplantation, test donor cells were considered to contain one or more multilineage repopulating cells.

HSC purification and transplantation

BM or spleen cells were suspended in PBS. Low-density cells (< 1.077 g/mL) were isolated using Ficoll-Paque PLUS (GE Healthcare, Little Chalfont, England). Cells were suspended in 0.05% sodium azide and 3% fetal calf serum in PBS and were stained with a lineage antibody mix consisting of biotinylated anti–Gr-1, -Mac1, -B220, -CD4, -CD8, -Ter119, and –interleukin-7 receptor antibodies (BD Biosciences). Lineage marker–positive cells were depleted using magnetic beads (Miltenyi Biotec, Bergisch Gladbach, Germany). Cells were stained with fluorescein isothiocyanate–conjugated anti-CD34, APC-conjugated anti–c-Kit, PE-conjugated anti–Sca-1, and the lineage antibody-mix antibodies. The biotinylated antibodies were developed with streptavidin–APC-Cy7. Flow cytometric analysis and sorting were performed on a MoFlo flow cytometer equipped with solid (488 nm) and HeNe (633 nm) lasers (Beckman Coulter, Fullerton, CA, USA). Cells were sorted by flow cytometry into screw-cap tubes (Ina Optica, Osaka, Japan) containing 1 mL of 10% fetal calf serum in α–minimal essential medium (Invitrogen, Tokyo, Japan). Cells were mixed with competitor cells at a desired ratio (e.g., 100 $CD34^-$KSL cells: 2×10^5 competitor cells). For single-cell transplantation, $CD34^-$KSL cells were individually sorted into each well of a 96-well plate, followed by addition of 2×10^5 competitor cells/well. Cells in 200 μL medium were injected into each of a group of lethally irradiated mice. To perform secondary transplantation, BM cells collected from each femur of all recipient mice were pooled. Each secondary mouse received BM cells equivalent to one-quarter of the total femoral BM of a primary recipient mouse. Peripheral blood cells of the recipient mice were analyzed 12 weeks after transplantation.

Single-cell colony assays

$CD34^-$KSL cells were sorted into a 96-well plate at one cell per well. Each well contained 200 μL 10% fetal calf serum, 1% bovine serum albumin, 5×10^{-5} M 2β-mercaptoethanol, 10 ng/mL mouse stem cell factor, 10 ng/mL human thrombopoietin, 10 ng/mL mouse interleukin-3, and 2 U/mL human erythropoietin in 200 μL α–minimum essential medium. On day 14 of culture, individual colonies were cytocentrifuged onto glass slides and stained with Hemacolor (Merck, Whitehouse Station, NJ, USA). Cells composing colonies were morphologically classified using light microscopy.

Parabiosis

A B6-Ly5.1 mouse and a B6-Ly5.2 mouse were surgically connected subcutaneously as described [17]. Using pentobarbital anesthesia, two mice underwent unilateral flank skin incisions from elbow to knee joints in mirror image. Mouse-to-mouse skin closure was achieved with an AUTOCLIP Wound Clip Applier using 9-mm clips (BD Biosciences).

Cell-cycle analysis

Lineage-depleted BM cells were suspended in PBS at 1×10^6 cells per milliliter and were incubated with 1 μg/mL pyronin Y (Sigma Aldrich Japan, Tokyo, Japan) at 37°C for 45 minutes. Cells were stained with antibodies as described here, except PE-anti–Sca-1 antibody (replaced by PE-Cy5.5-anti–Sca-1 antibody). Cells were analyzed by FACS Vantage SE or Aria II (BD Biosicences) flow cytometry.

To analyze in vivo cell-cycle kinetics of HSCs, bromodeoxyuridine (BrdU; Sigma-Aldrich Japan) was added to mouse water bottles at 0.5 mg/mL for 3, 7, 14, or 21 days before sacrifice. $CD34^-$KSL cells purified from BM or spleen were fixed with 70% ethanol at −30°C overnight. After washing, cells were suspended in 25 μL 4M HCl and 0.5% Tween 20 in water at room temperature for 30 minutes. After 300 μL Tris-HCl (pH 8.0) was added, cells were centrifuged. Cells were stained with Alexa 488–conjugated anti-BrdU antibody (Invitrogen) at room temperature for 90 minutes. RNase and propidium iodide were added at 15 μg/mL and 5 μg/mL, respectively. Cells were analyzed by FACSCalibur flow cytometry (BD Biosciences). Alternatively, $CD34^-$KSL cells were directly sorted by flow cytometry into a droplet on a poly-L-Lys–coated glass slide. Single-cell immunostaining was performed as described [18]. In brief, glass slides were placed in a staining jar containing 100% ethanol for 60 minutes at −30°C. Cells were fixed with 4% paraformaldehyde for 10 minutes and treated with 4N HCl for 10 minutes. Cells were reacted with Alexa 488–conjugated anti-BrdU antibody overnight. After counterstaining with TOTO3 iodide (Invitrogen), cells were analyzed with Arrayscan (Thermo Fisher Scientific, Waltham, MA, USA).

Results

Repopulating activity in spleen cells is lower than that in BM cells

BM or spleen cells (1×10^6 cells) were mixed with BM competitor cells (1×10^6 cells) and the mixture was transplanted into individual lethally irradiated mice. Long-term

multilineage reconstitution was evaluated 16 weeks after transplantation (Fig. 1A and Supplementary Figure E1 [online only, available at www.exphem.org]). As expected, the mean percent chimerism achieved by BM cells was around 50%. However, that achieved by spleen cells was only 6.5%. These data are in good agreement with previous observations that more spleen cells than BM cells are required to reach the same level of repopulation [19]. To evaluate the repopulating activity in a quantitative fashion, the percentage of chimerism was transformed to RU [15]. RU values per 10^6 BM cells or spleen cells were 11.2 or 0.75, respectively. Thus, BM cells had about 15 times as many RU per 10^6 cells as did spleen cells. As shown in Supplementary Figure E1 (online only, available at www.exphem.org), while all myeloid, B-lymphoid, and T-lymphoid lineages were reconstituted by BM cells in every recipient mouse, lymphoid lineages were predominantly reconstituted by spleen cells in four of nine recipient mice. Because we did not observe this sort of lymphoid reconstitution when transplanting whole BM cells, this may have been because only the spleen contained particular B and T lymphocytes capable of surviving for a long time after transplantation. If this is the case, our spleen-cell RU values may be somewhat overestimated.

Frequency of repopulating cells in spleen cells is lower than that in BM cells

In vivo limiting dilution-type analysis was performed to estimate the frequency of repopulating cells in BM or spleen cells. Graded numbers of test donor BM or spleen cells were transplanted in competitive settings. As shown in Figure 1B, the frequency of long-term repopulating cells (LTRCs) in BM was about 1 in 3×10^4 cells, consistent with previous observations [20,21]. On the other hand, that frequency in spleen was about 1 in 3.1×10^5 cells. We examined the frequency of LTRCs in the spleen in another experiment. It was about 1 in 7.3×10^5 cells (data not shown). Thus, the frequency of LTRCs in the spleen was estimated as 1 in 3.1 to 7.3×10^5 cells (on average, $1/5.2 \times 10^5$ cells).

RU, calculated using the percentage of chimerism, represent the amount of repopulating activity in test donor cells [15]. Competitive repopulating units (CRU), determined by limiting dilution assay, represent the number of repopulating cells in test donor cells [16]. The more CRU that are transplanted, the higher the percentages of chimerism or RU obtained. Each CRU has a variety of RU [20], but one can compare the mean RU per single CRU. The mean activity per stem cells (MAS) is defined as (RU per test donor cells) divided by (CRU per test donor cells) [21]. When MAS values are similar for the same numbers of test donor cells from different sources, one can assume that stem cell qualities in these different sources are, on average, similar. BM MAS was 0.34, consistent with previous observations [21]. Spleen MAS was 0.39. Allowing for slight overestimation of spleen RU values, these data suggest that repopulating activity in spleen HSCs, on average, is similar to that in BM HSCs.

Isolation of LTRCs from spleen

CD34-negative/low, c-Kit–positive, Sca-1–positive, lineage marker–negative ($CD34^-KSL$) cells are highly enriched in adult BM HSCs [22]. We asked whether cells with the same markers are similarly enriched in adult spleen HSCs. BM and spleen cells from the same mice were stained with

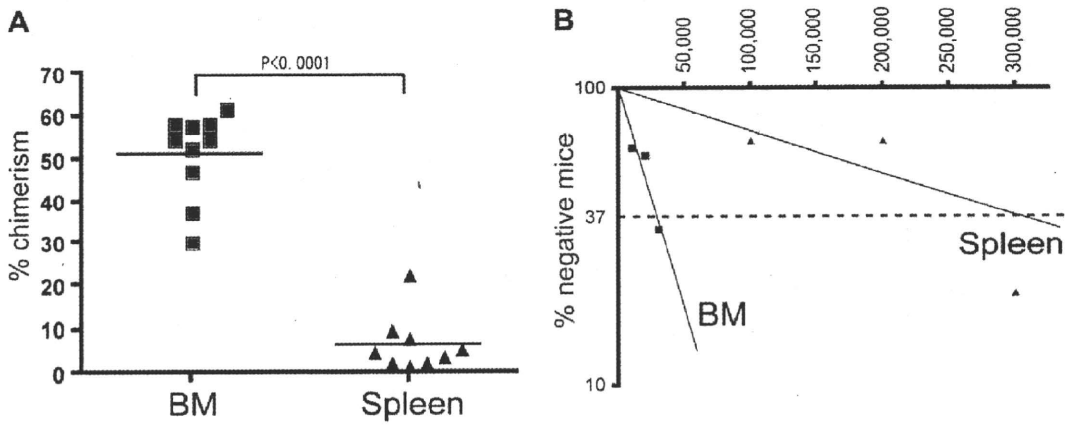

Figure 1. LTRCs in mouse BM or spleen. Two types of competitive repopulating assays were performed on BM and spleen cells from adult mice as described [21,32]. Recipient mice were analyzed 16 weeks after transplantation. (**A**) A mixture of 1×10^6 test donor BM or spleen cells and 1×10^6 BM cells was transplanted into each of 10 lethally irradiated mice. Transplantation of BM cells resulted in 51.3% ± 10.2% percent chimerism (mean ± SD, n = 10). Transplantation of spleen cells resulted in 6.5% ± 6.4% percent chimerism (mean ± SD, n = 9 [one mouse died before analysis]). The percent chimerism conferred by BM cells was significantly greater than that conferred by spleen cells (unpaired *t*-test with Welch correction). See Supplementary Figure E1 (online only, available at www.exphem.org) for myeloid, B-lymphoid, and T-lymphoid lineage reconstitution by BM or spleen cells. (**B**) By limiting dilution assay, the frequency of LTRCs was estimated to be 1 in 29,229 BM cells (95% confidence interval, 1/17,048–1/50,113) or 1 in 307,354 spleen cells (95% confidence interval, 1/158,070–1/597,624).

antibodies and analyzed by flow cytometry (Fig. 2). CD34$^-$KSL cells accounted for 0.005 ± 0.002 (mean ± standard deviation [SD], n = 4) of BM cells as reported [20–22] and accounted for 0.0004 ± 0.0004 (n = 4) of spleen cells. On the other hand, CD34$^+$KSL cells accounted for 0.14 ± 0.02 (n = 4) and 0.004 ± 0.001 (n = 4) of BM and spleen cells, respectively. To examine the function of CD34$^-$ or CD34$^+$KSL spleen cells, 100 cells from each fraction were transplanted into each of a group of lethally irradiated mice. As in BM, CD34$^-$KSL cells, but not CD34$^+$KSL cells in the spleen, were enriched in long-term repopulating activity (Supplementary Figure E2; online only, available at www.exphem.org). We decided to characterize spleen HSCs further by using CD34$^-$KSL cells as an HSC-enriched fraction.

Colony-forming activity in BM and spleen CD34$^-$KSL cells

As shown in Supplementary Figure E3 (online only, available at www.exphem.org), >90% of BM CD34$^-$KSL cells formed colonies in vitro as reported [23]. Although their colony-forming efficiency seemed slightly lower, >80% of spleen CD34$^-$KSL cells formed colonies in vitro. Colony-forming units with differentiation potential for all neutrophil, macrophage, erythrocyte, and megakaryocyte lineages, which is possibly another aspect of LTRC activity [23], were similarly detected in BM and spleen CD34$^-$KSL cells. These data support the concept that CD34$^-$KSL cells are similarly enriched in both BM and spleen HSCs of adult mice.

Competitive repopulation with BM and spleen CD34$^-$KSL cells

Competitive repopulating assays were performed on BM or spleen CD34$^-$KSL cells. Figure 3 shows data from transplantation of 10 CD34$^-$KSL cells and of single such cells. After 10 BM or spleen CD34$^-$KSL cells were transplanted, a variety of levels of percent chimerism was observed among individual recipient mice (Fig. 3A). Long-term reconstitution levels achieved by 10 spleen CD34$^-$KSL cells did not significantly differ on average from those achieved by 10 BM CD34$^-$KSL cells (Fig. 3A). In order to compare self-renewal potential, secondary transplantation was performed with BM cells pooled from all primary recipient mice. After secondary transplantation, levels of percent chimerism did not significantly differ between recipients of BM and spleen CD34$^-$KSL cells (Fig. 3B). These data show that repopulating and self-renewal potentials are similar in BM and spleen CD34$^-$KSL cells.

To confirm that the engraftment rates of LRTCs are also similar between BM and spleen CD34$^-$KSL cells, single-cell transplantation was performed. Transplantation of single BM or spleen CD34$^-$KSL cells resulted in long-term reconstitution in 9 of 29 or 7 of 29 recipient mice, respectively (Fig. 3C). Based on data from transplantation with 10 cells and single cells, we roughly estimated the frequency of LTRCs. The frequency of LTRCs in BM CD34$^-$KSL cells was about one in three cells, consistent with our previous observations [21], while that in spleen CD34$^-$KSL cells was

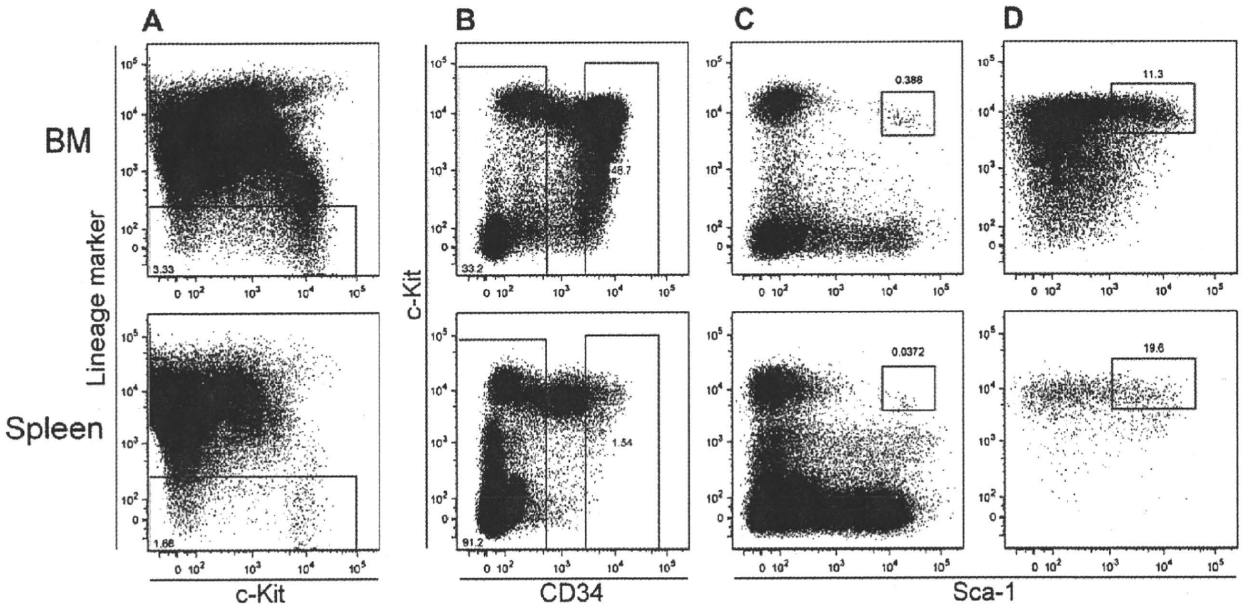

Figure 2. CD34$^-$KSL cells in BM and spleen. Lineage-depleted BM or spleen cells were stained with antibodies and analyzed on a flow cytometer. The upper and lower panels show BM analysis and spleen analysis, respectively. (**A**) Dot plots display expression of c-Kit and lineage markers with square gates for lineage-negative cells. (**B**) Dot plots display expression of CD34 and c-Kit in lineage-negative cells with square gates for CD34$^{-/low}$ or CD34$^+$ lineage-negative cells. (**C**) Dot plots display expression of Sca-1 and c-Kit in CD34$^{-/low}$ lineage-negative cells with square gates for CD34$^-$KSL cells. (**D**) Dot plots display expression of Sca-1 and c-Kit in CD34$^+$ lineage-negative cells with square gates for CD34$^+$KSL cells.

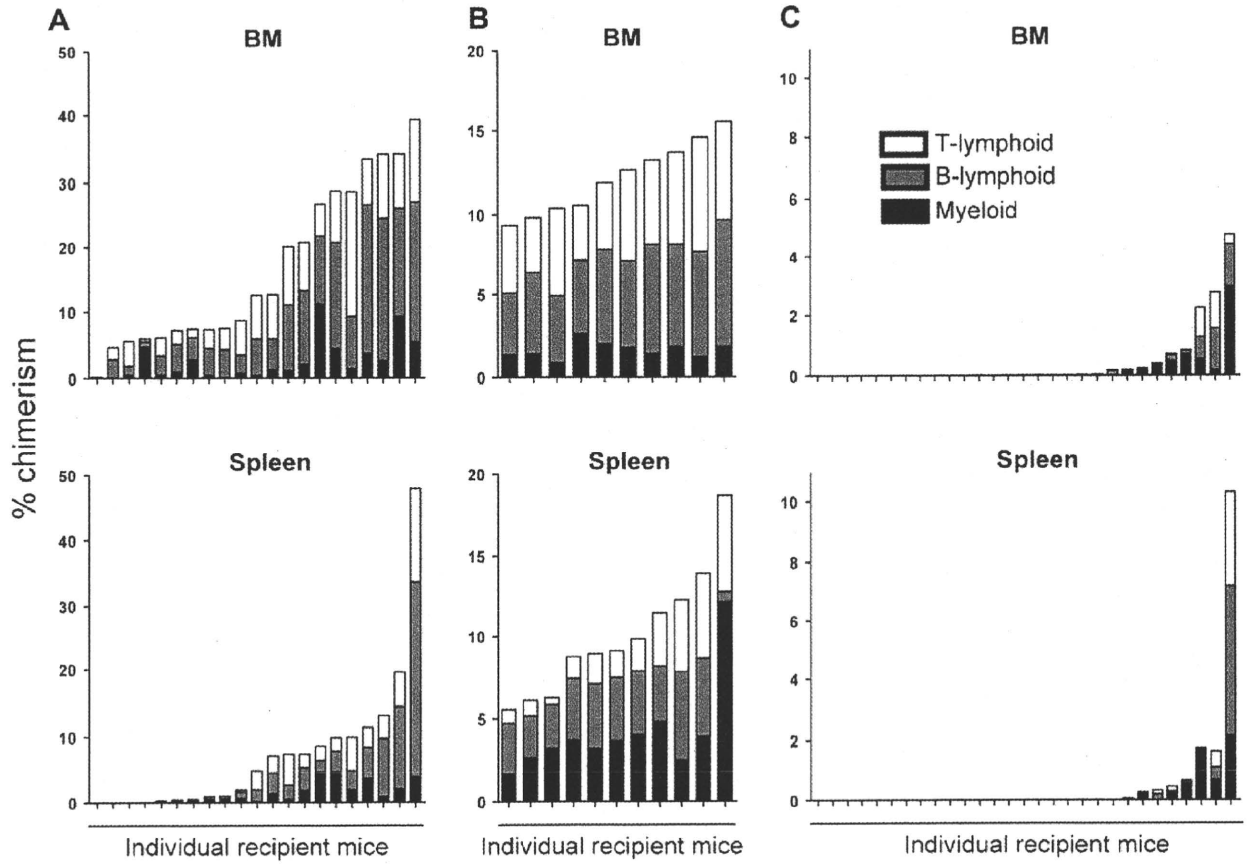

Figure 3. Long-term reconstitution by 10 BM or spleen CD34$^-$KSL cells or by individual such cells. (**A**) 10 CD34$^-$KSL cells from BM or spleen were transplanted into each of 21 lethally irradiated mice, together with 2×10^5 BM cells. Recipient mice were analyzed 16 weeks after transplantation. Each column represents percent chimerism (consisting of myeloid, B-lymphoid, and T-lymphoid lineages). Percent chimerism was 16.7% ± 12.3% (mean ± SD, n = 21) for BM CD34$^-$KSL cells and 9.0% ± 11.3% (n = 17) for spleen CD34$^-$KSL cells. (**B**) Secondary transplantation was performed with pooled bone marrow cells from all primary recipient mice. Recipient mice were analyzed 13 weeks after transplantation. Percent chimerism was 12.3% ± 2.1% (n = 10) for cells derived from BM CD34$^-$KSL cells and 9.8% ± 4.0% (n = 11) for cells derived from spleen CD34$^-$KSL cells. (**C**) Single CD34$^-$KSL cells from BM or spleen were transplanted into each of 30 lethally irradiated mice, together with 2×10^5 BM cells. Recipient mice were analyzed 12 weeks after transplantation. Each column represents percent chimerism. One mouse in each group died before analysis. Of 29 recipient mice, 9 and 7 were reconstituted with single BM or spleen CD34$^-$KSL cells, respectively. Recipient mice with >0.1% chimerism for one or more lineages are shown.

about one in five cells. These data did not permit statistical analysis. If a large number of single cells were transplanted or limiting dilution type of experiments were performed, a significant difference in frequency of LTRCs between BM and spleen CD34$^-$KSL cells would be obtained. However, such a difference should be only trivial. Predominant lymphoid reconstitution, seen after transplantation with whole spleen cells (Supplementary Figure E1; online only, available at www.exphem.org), was never detected after transplantation with spleen CD34$^-$KSL cells (Fig. 3). These data support the possibility that lymphoid repopulating cells other than HSCs are present in the spleen.

Spleen HSCs differ from circulating HSCs

As blood flow through the spleen is abundant, transiently circulating HSCs could have been detected as spleen HSCs. In order to address this issue, a parabiosis model was used in which cross-circulation was established in B6-Ly5.1:B6-Ly5.2 mouse pairs. Five pairs of mice could be analyzed at 7 or 14 weeks of parabiosis (Fig. 4). In B6-Ly5.1 mice, 49.4% ± 4.4% (mean ± SD, n = 5) of peripheral blood cells were replaced by Ly5.2 cells. In B6-Ly5.2 mice, 39.2% ± 11.4% (mean ± SD, n = 5) of peripheral blood cells were replaced by Ly5.1 cells. These data confirmed near-equal mixing of peripheral blood in parabiosis [17]. All the following figures were calculated on the same basis. In B6-Ly5.1 mice, 20.4% ± 8.8% of whole BM cells were replaced by Ly5.2 cells. In B6-Ly5.2 mice, 20% ± 14.0% of whole BM cells were replaced by Ly5.1 cells. Interestingly, more cells were replaced by partner-derived cells in the spleen: In B6-Ly5.1 mice, 44.9% ± 7.1% of whole spleen cells were replaced by Ly5.2 cells, and in B6-Ly5.2 mice,

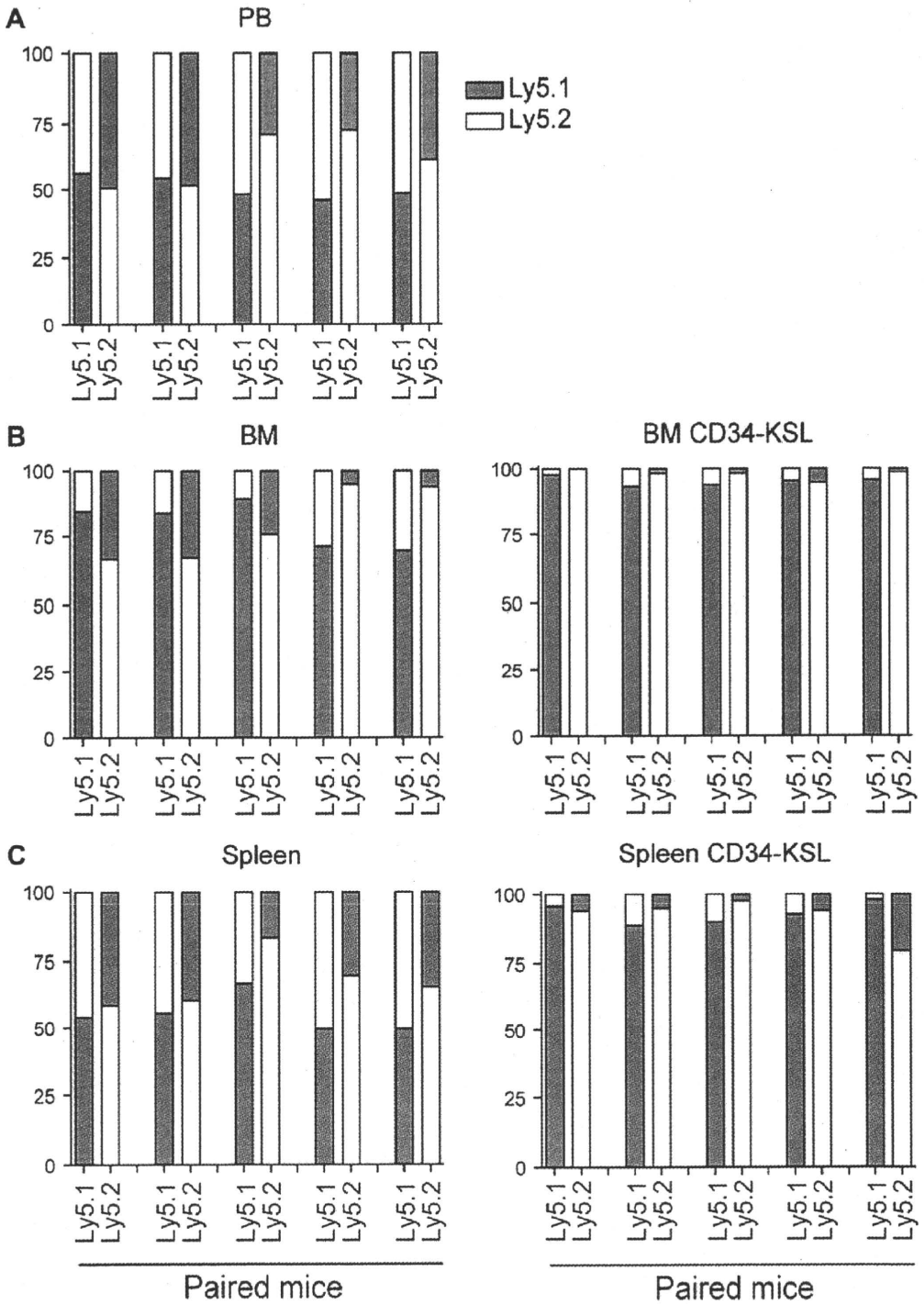

Figure 4. Analysis of parabiotic mice. (**A**) Peripheral blood cells of paired mice were analyzed for endogenous and partner-derived cells. (**B**) Whole BM cells (left panel) and BM CD34$^-$KSL cells (right panel) of paired mice were analyzed for endogenous and partner-derived cells. (**C**) Whole spleen cells (left panel) and spleen CD34$^-$KSL cells (right panel) of paired mice were analyzed for endogenous and partner-derived cells. B6-Ly5.1 mice were paired with B6-Ly5.2 mice. The pairs of mice were numbered 1-5 from left to right. Three pairs of mice (nos. 1, 2, and 3) were analyzed at 7 weeks of parabiosis. Two pairs of mice (nos. 4 and 5) were analyzed at 14 weeks of parabiosis. Pair no. 4 consisted of two male mice. The remaining pairs each consisted of two female mice.

32.5% ± 9.7% of whole spleen cells were replaced by Ly5.1 cells. These data show that, in parabiotic settings, a proportion of whole BM cells is exchangeable with cells from the circulation, and that most whole spleen cells become indistinguishable from peripheral blood cells after a certain interval.

With respect to the HSC population in parabiosis, significantly fewer cells were replaced by partner-derived cells. In B6-Ly5.1 mice, 6.6% ± 3.0% of BM CD34$^-$KSL cells and 8.6% ± 4.2% of spleen CD34$^-$KSL cells were replaced by Ly5.2 cells. In B6-Ly5.2 mice, 2.4% ± 1.7% of BM CD34$^-$KSL cells and 9.2% ± 6.4% of spleen CD34$^-$KSL cells were replaced by Ly5.2 cells. In contrast to the good numbers of unfractionated cells in BM and spleen that exchange places with their circulating counterparts, only small proportions of HSCs in BM and spleen exchange places with circulating HSCs. These data overall suggest that most spleen HSCs are long-term residents in the spleen.

Cell-cycle analysis of BM and spleen CD34$^-$KSL cells

Most adult HSCs are considered to be quiescent at any one time [24]. BM and spleen CD34$^-$KSL cells were stained with pyronin Y and were analyzed by flow cytometry (Fig. 5A). Pyronin Y^{low} cells were considered to be in the G_0 phase of the cell cycle (G_0 cells). Figure 5A shows representative data for G_0 cells among BM or spleen CD34$^-$KSL cells. G_0 cells accounted for 97.9% ± 1.5% (mean ± SD, n = 8) of BM CD34$^-$KSL cells, or 90.9 ± 5.2 (n = 8) of spleen CD34$^-$KSL cells. Paired *t*-testing showed significant differences between the two groups ($p = 0.0015$). These data suggest that spleen CD34$^-$KSL cells are more frequently in cycle than are BM CD34$^-$KSL cells.

To compare cell-cycle kinetics between BM and spleen CD34$^-$KSL cells, in vivo BrdU labeling was performed (Supplementary Figure E4; online only, available at www.exphem.org). The mean turnover time has been defined as the time point when BrdU-negative cells compose 37% of the cells analyzed and the 50% turnover time ($t_{1/2}$) has been defined as the time point when BrdU-negative cells compose 50% of the cells analyzed [25]. As shown in Figure 5B, the $t_{1/2}$ turned out to be approximately 17 days or 9 days for BM or spleen CD34$^-$KSL cells, respectively. The mean turnover time of BM CD34$^-$KSL cells was estimated to be approximately 25 days, consistent with previous observations [20,25]. In contrast, the mean turnover time of spleen CD34$^-$KSL cells was estimated to be approximately 13 days. The mean G_0 time was defined as (mean turnover time) minus (mean cell cycle time) when the G_0 concept was originally proposed by Lajtha [26]. The mean cell cycle time in HSCs is not yet determined precisely. The mean cell cycle time is presumably much shorter than the mean turnover time in HSCs, and cycling time does not differ between BM and spleen HSCs. The difference in the mean turnover time should arise largely from the difference in the mean G_0 time. These data show that spleen CD34$^-$KSL cells cycle almost twice as often as do BM CD34$^-$KSL cells.

Of interest was to know whether cell cycling in BM or spleen HSCs is determined cell intrinsically or cell extrinsically. To assess this, lethally irradiated mice were transplanted with BM or spleen cells. Mice were analyzed 12 months after transplantation. Mice were given BrdU for 1 week. BrdU uptake by CD34$^-$KSL cells was analyzed with Arrayscan in this series of experiments to permit reduction in the number of cells required for analysis. Analysis of BM or spleen CD34$^-$KSL cells from normal mice showed that spleen CD34$^-$KSL cells entered the cell cycle more frequently than did BM CD34$^-$KSL cells (Supplementary Figure E5A; online only, available at www.exphem.org), consistent with data from flow cytometric analysis (Supplementary Figure E4; online only, available at www.exphem.org). In reconstituted mice, regardless of the sources of donor HSCs, spleen CD34$^-$KSL cells were in cycle more frequently than were BM CD34$^-$KSL cells (Supplementary Figure E5B, C; online only, available at www.exphem.org). These data suggest organ-specific regulation for HSC cycling.

Discussion

This is the first study to show that spleen HSCs are phenotypically and functionally similar to BM HSCs. Data from both CRU assays (Fig. 1) and phenotypic analysis combined with reconstitution assays (Figs. 2, 3) showed that the frequency of HSCs in the spleen is significantly lower than that in the BM. However, data from both MAS estimation and single-cell transplantation (Fig. 3) showed that stem cell activity per cell is similar between BM and spleen HSCs. The functional similarity of BM and spleen HSCs raised the possibility that they interchange sites via the circulation. Parabiosis data (Fig. 4) suggested that most BM HSCs and spleen HSCs are long-term residents in each organ.

This study suggests that G_0 length differs between BM and spleen HSCs. Data from both pyronin Y staining and BrdU-uptake analysis (Fig. 5) indicate that spleen HSCs enter the cell cycle more frequently than do HSCs. The mean turnover time of BM HSCs was estimated to be about twice as long as that in spleen HSCs, suggesting that quiescence in BM HSCs is longer than in spleen HSCs. Interestingly, this was the case for BM and spleen HSCs in mice that had previously been reconstituted with BM or spleen cells (Supplementary Figure E5; online only, available at www.exphem.org). The duration of quiescence in HSCs might be regulated in an organ-specific manner. These data support the concept that the maintenance of quiescence in HSCs is a function of the HSC niche. Recently, the cell cycle of circulating HSCs was analyzed; BrdU uptake kinetics were reportedly similar in BM and PB HSCs

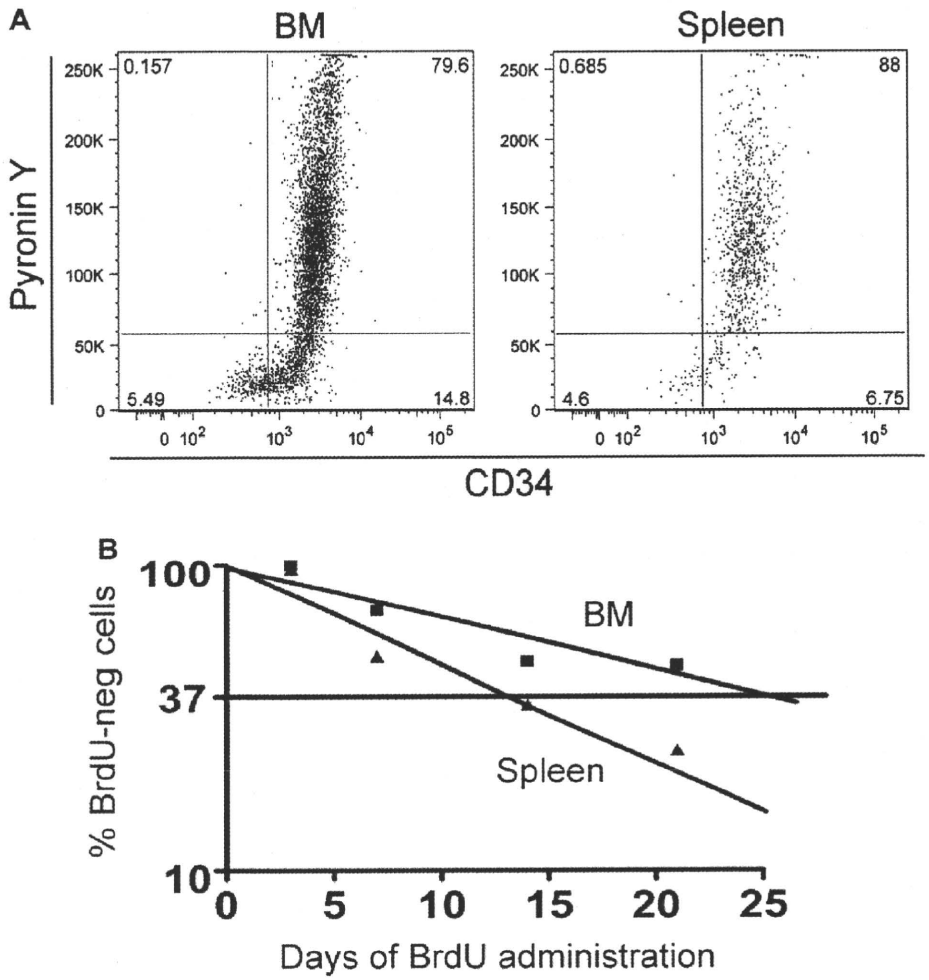

Figure 5. Cell-cycle analysis for BM or spleen CD34$^-$KSL cells. (**A**) CD34$^-$KSL cells were stained with pyronin Y. The representative flow cytometry profiles show CD34 expression and pyronin Y staining intensity in BM and spleen KSL cells. (**B**) The semi-log plot shows percent BM and spleen CD34$^-$KSL cells lacking BrdU uptake. BM data significantly differed from spleen data ($p < 0.0001$). The mean turnover times were approximately 13 days or 25 days for spleen or BM CD34$^-$KSL cells, respectively. The 50% turnover times were approximately 9 or 17 days for spleen or BM CD34$^-$KSL cells, respectively.

[27]. In this study, the kinetics of BrdU uptake differed between spleen and BM HSCs. We infer that the kinetics of BrdU uptake also should differ between spleen and PB HSCs, supporting our conclusion that most spleen HSCs do not readily exchange places with circulating HSCs.

Osteoblasts have been proposed as a constituent of the BM niche [7–9], and endochondral ossification is reportedly required for niche formation [28]. Vascular endothelial cells are another good candidate for niche constituent cells [10]. The spleen niche is supposedly composed of vascular endothelial cells but not of osteoblasts. Difference in cell-cycle coordination for large numbers of HSCs may result from distinct niche components in each organ. If this is the case, osteogenesis-related elements should play a role in prolonging quiescence in BM HSCs and not in spleen HSCs. Of importance, however, is that HSC quiescence takes place regardless of the absence of osteoblasts. If niche itself is similar between BM and spleen, to postulate a control center for widely distributed niches (in BM or spleen) may be necessary. Such a center would signal to BM and spleen niches in different manners.

We do not know how and to what extent spleen HSCs contribute to hematopoiesis under physiological conditions. Spleen HSCs seem not to differentiate in the same way as BM HSCs. Differentiation pathways from spleen HSCs possibly differ from those of BM HSCs. Because differentiation pathways for BM HSCs are still debated [29,30], it is interesting to compare road maps of differentiation between BM and spleen HSCs. Rapid erythropoiesis takes place in mouse spleen when acute hemolytic anemia is induced by phenylhydrazine [31]. The spleen may serve as a reservoir of HSCs for relatively immediate use. In this regard, a short

G_0 time may work as an advantage for spleen HSCs so that they can give rise to progeny with little delay.

Acknowledgments

We are grateful to Dr. A. S. Knisely for critical review of the manuscript. This work was supported by grants from the Ministry of Education, Culture, Sport, Science, and Technology, Japan.

Conflict of interest disclosure

No financial interest/relationships with financial interest relating to the topic of this article have been declared.

References

1. Metcalf D, Moore MAS. Haemopoietic cells. Amsterdam: North-Holland Publishing Co; 1971.
2. Christensen JL, Wright DE, Wagers AJ, Weissman IL. Circulation and chemotaxis of fetal hematopoietic stem cells. PLoS Biol. 2004;2:E75.
3. Gekas C, Dieterlen-Lievre F, Orkin SH, Mikkola HK. The placenta is a niche for hematopoietic stem cells. Dev Cell. 2005;8:365–375.
4. Ottersbach K, Dzierzak E. The murine placenta contains hematopoietic stem cells within the vascular labyrinth region. Dev Cell. 2005; 8:377–387.
5. Schofield R. The relationship between the spleen colony-forming cell and the haemopoietic stem cell. Blood Cells. 1978;4:7–25.
6. Kiel MJ, Morrison SJ. Uncertainty in the niches that maintain haematopoietic stem cells. Nat Rev Immunol. 2008;8:290–301.
7. Zhang J, Niu C, Ye L, et al. Identification of the haematopoietic stem cell niche and control of the niche size. Nature. 2003;425:836–841.
8. Calvi LM, Adams GB, Weibrecht KW, et al. Osteoblastic cells regulate the haematopoietic stem cell niche. Nature. 2003;425:841–846.
9. Arai F, Hirao A, Ohmura M, et al. Tie2/angiopoietin-1 signaling regulates hematopoietic stem cell quiescence in the bone marrow niche. Cell. 2004;118:149–161.
10. Kiel MJ, Yilmaz OH, Iwashita T, Yilmaz OH, Terhorst C, Morrison SJ. SLAM family receptors distinguish hematopoietic stem and progenitor cells and reveal endothelial niches for stem cells. Cell. 2005;121:1109–1121.
11. Sugiyama T, Kohara H, Noda M, Nagasawa T. Maintenance of the hematopoietic stem cell pool by CXCL12-CXCR4 chemokine signaling in bone marrow stromal cell niches. Immunity. 2006;25: 977–988.
12. Sacchetti B, Funari A, Michienzi S, et al. Self-renewing osteoprogenitors in bone marrow sinusoids can organize a hematopoietic microenvironment. Cell. 2007;131:324–336.
13. Morikawa S, Mabuchi Y, Kubota Y, et al. Prospective identification, isolation, and systemic transplantation of multipotent mesenchymal stem cells in murine bone marrow. J Exp Med. 2009;206:2483–2496.
14. Mendez-Ferrer S, Michurina TV, Ferraro F, et al. Mesenchymal and haematopoietic stem cells form a unique bone marrow niche. Nature. 2010;466:829–834.
15. Harrison DE, Jordan CT, Zhong RK, Astle CM. Primitive hemopoietic stem cells: direct assay of most productive populations by competitive repopulation with simple binomial, correlation and covariance calculations. Exp Hematol. 1993;21:206–219.
16. Szilvassy SJ, Humphries RK, Lansdorp PM, Eaves AC, Eaves CJ. Quantitative assay for totipotent reconstituting hematopoietic stem cells by a competitive repopulation strategy. Proc Natl Acad Sci U S A. 1990;87:8736–8740.
17. Wright DE, Wagers AJ, Gulati AP, Johnson FL, Weissman IL. Physiological migration of hematopoietic stem and progenitor cells. Science. 2001;294:1933–1936.
18. Ema H, Morita Y, Yamazaki S, et al. Adult mouse hematopoietic stem cells: purification and single-cell assays. Nat Protoc. 2006;1:2979–2987.
19. Harrison DE, Zsebo KM, Astle CM. Splenic primitive hematopoietic stem cell (PHSC) activity is enhanced by steel factor because of PHSC proliferation. Blood. 1994;83:3146–3151.
20. Sudo K, Ema H, Morita Y, Nakauchi H. Age-associated characteristics of murine hematopoietic stem cells. J Exp Med. 2000;192:1273–1280.
21. Ema H, Sudo K, Seita J, et al. Quantification of self-renewal capacity in single hematopoietic stem cells from normal and Lnk-deficient mice. Dev Cell. 2005;8:907–914.
22. Osawa M, Hanada K, Hamada H, Nakauchi H. Long-term lymphohematopoietic reconstitution by a single CD34-low/negative hematopoietic stem cell. Science. 1996;273:242–245.
23. Takano H, Ema H, Sudo K, Nakauchi H. Asymmetric division and lineage commitment at the level of hematopoietic stem cells: inference from differentiation in daughter cell and granddaughter cell pairs. J Exp Med. 2004;199:295–302.
24. Yamazaki S, Iwama A, Takayanagi S, et al. Cytokine signals modulated via lipid rafts mimic niche signals and induce hibernation in hematopoietic stem cells. EMBO J. 2006;25:3515–3523.
25. Bradford GB, Williams B, Rossi R, Bertoncello I. Quiescence, cycling, and turnover in the primitive hematopoietic stem cell compartment. Exp Hematol. 1997;25:445–453.
26. Lajtha LG. Stem cell concepts. Differentiation. 1979;14:23–34.
27. Bhattacharya D, Czechowicz A, Ooi AG, Rossi DJ, Bryder D, Weissman IL. Niche recycling through division-independent egress of hematopoietic stem cells. J Exp Med. 2009;206:2837–2850.
28. Chan CK, Chen CC, Luppen CA, et al. Endochondral ossification is required for haematopoietic stem-cell niche formation. Nature. 2009; 457:490–494.
29. Adolfsson J, Mansson R, Buza-Vidas N, et al. Identification of Flt3+ lympho-myeloid stem cells lacking erythro-megakaryocytic potential a revised road map for adult blood lineage commitment. Cell. 2005; 121:295–306.
30. Arinobu Y, Mizuno S, Chong Y, et al. Reciprocal activation of GATA-1 and PU.1 marks initial specification of hematopoietic stem cells into myeloerythroid and myelolymphoid lineages. Cell Stem Cell. 2007;1: 416–427.
31. Vannucchi AM, Paoletti F, Linari S, et al. Identification and characterization of a bipotent (erythroid and megakaryocytic) cell precursor from the spleen of phenylhydrazine-treated mice. Blood. 2000;95: 2559–2568.
32. Ema H, Nakauchi H. Expansion of hematopoietic stem cells in the developing liver of a mouse embryo. Blood. 2000;95:2284–2288.

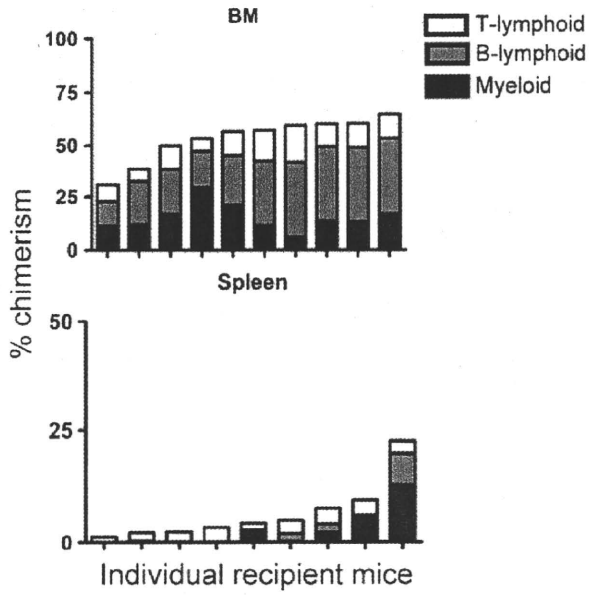

Supplementary Figure E1. Lineage reconstitution by whole BM or spleen cells Competitive repopulation was performed using whole BM or spleen cells. Recipient mice were analyzed 16 weeks after transplantation. Myeloid, B-lymphoid, and T-lymphoid lineage reconstitution are shown for individual recipient mice.

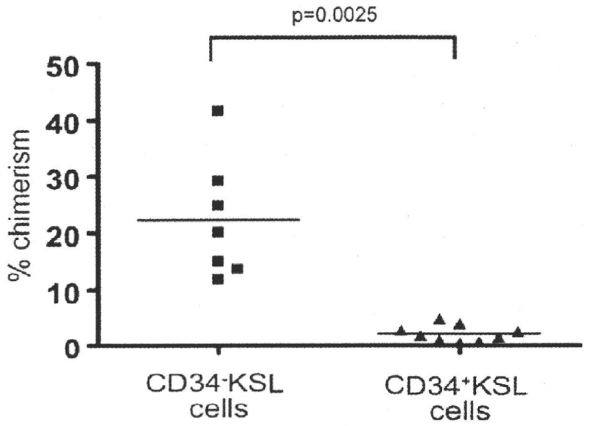

Supplementary Figure E2. CD34$^-$KSL cells are enriched in spleen HSC activity Individual lethally irradiated mice were transplanted with 100 CD34$^-$ or CD34$^+$KSL cells isolated from spleen along with 2×10^5 BM competitor cells. Recipient mice were analyzed 16 weeks after transplantation. Percent chimerism conferred by CD34$^-$ and CD34$^+$KSL cells was 22.3 ± 10.6 (mean ± SD, n = 7) or 2.2 ± 1.5 (n = 9), respectively. Unpaired *t*-testing (with Welch correction) showed a significant difference between the groups ($p = 0.0025$).

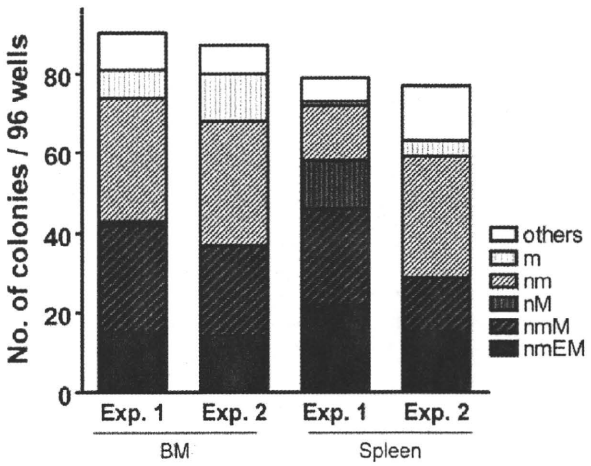

Supplementary Figure E3. Single-cell cultures with CD34$^-$KSL BM or spleen cells CD34$^-$KSL cells from BM or spleen were individually sorted into each well of a 96-well microtiter plate. Cells were cultured for 14 days in the presence of stem cell factor, thrombopoietin, interleukin-3, and erythropoietin. Cytocentrifugation was performed on each colony to permit light-microscopy morphological examination of colony-composing cells. Data from two individual experiments are shown. E = erythroblasts; m = macrophages; M = megakaryocytes; n = neutrophils.

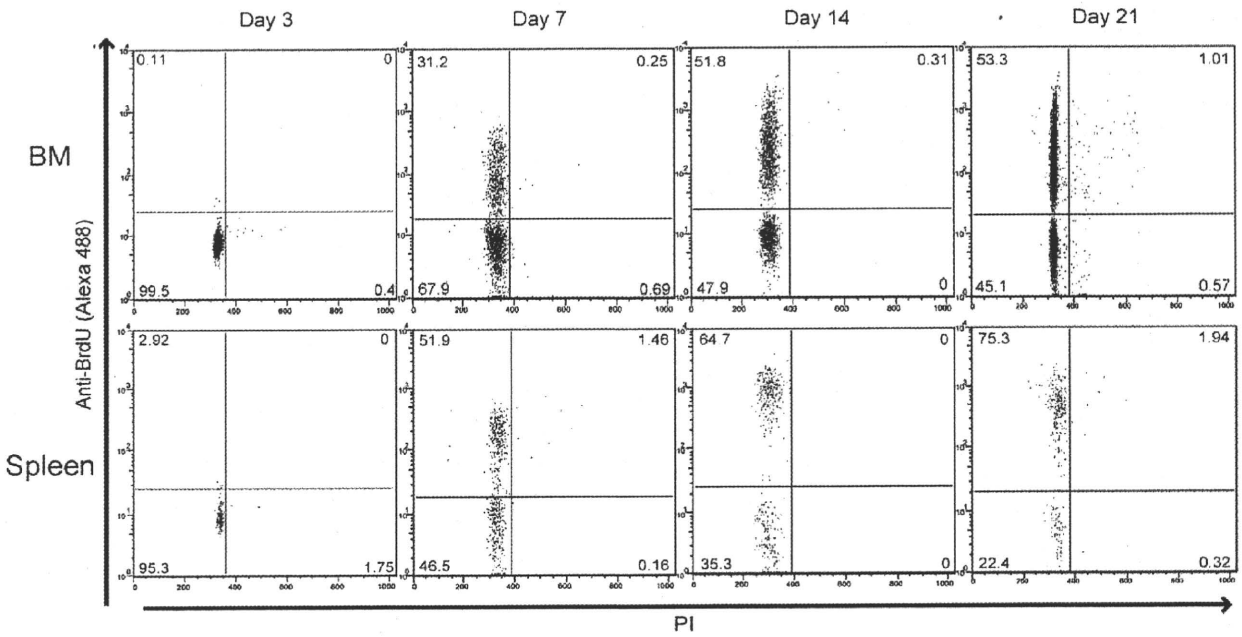

Supplementary Figure E4. Flow cytometric analysis of BrdU uptake by $CD34^{-}KSL$ cells. Groups of 10 mice received BrdU in drinking water for 3, 7, 14, or 21 days. BM and spleen cells obtained from each group of mice were pooled. $CD34^{-}KSL$ cells isolated from pooled BM or spleen cells were stained with anti-BrdU antibody, followed by propidium iodide (PI) staining. The upper and lower panels show BM and spleen cells, respectively. These data are graphically presented in Figure 5B.

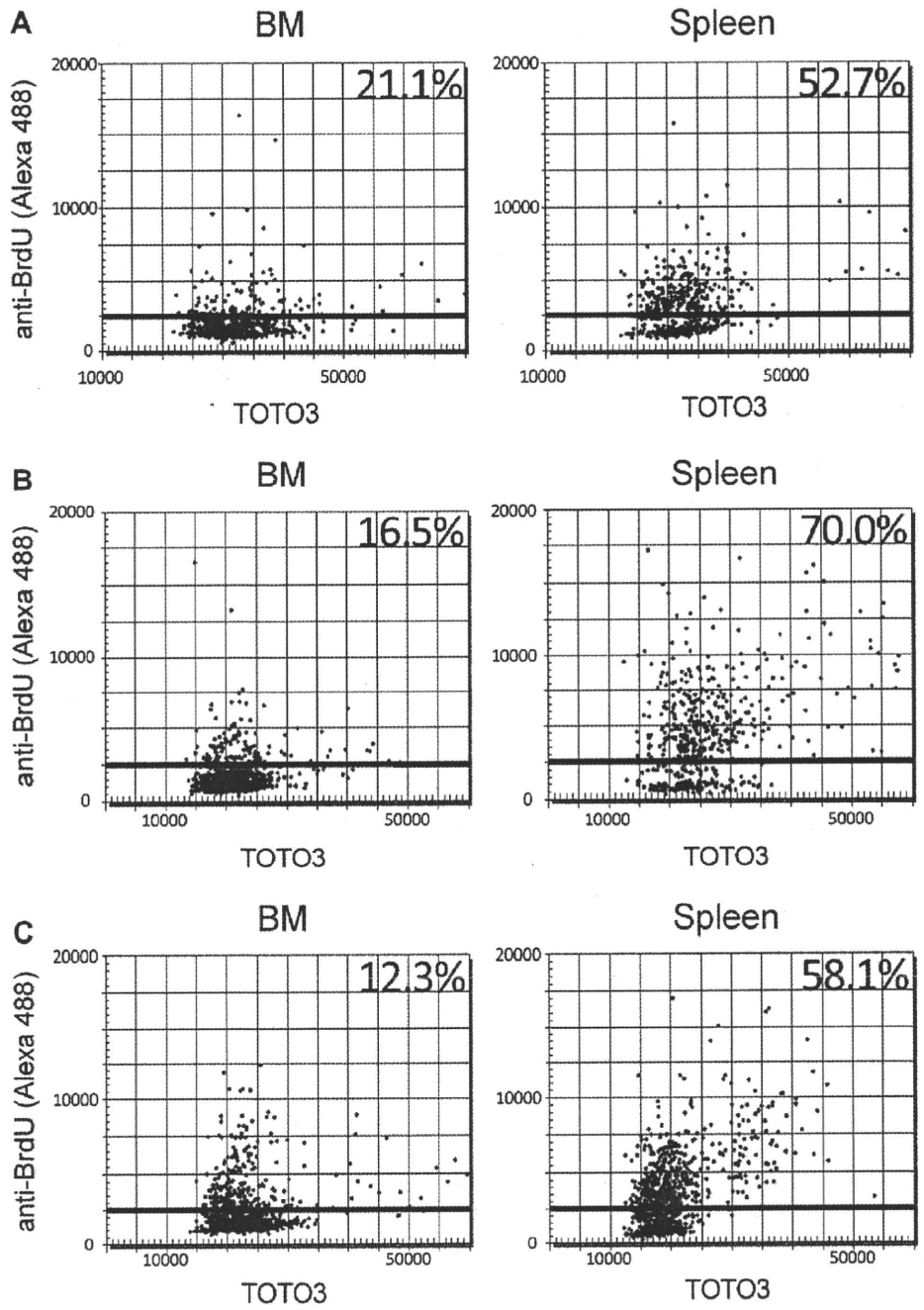

Supplementary Figure E5. Arrayscan analysis of BrdU uptake by $CD34^{-}KSL$ cells. Groups of 3 to 5 mice received BrdU in drinking water for 7 days; 1000 to 2000 BM and spleen CD34-KSL cells were isolated from each group and placed on glass slides. After staining with anti-BrdU antibody and TOTO3, 500 to 1000 cells were analyzed and data were collected with Arrayscan. (**A**) BM or spleen $CD34^{-}KSL$ cells from normal mice were analyzed. (**B**) Lethally irradiated mice (Ly5.2) were transplanted with 1×10^6 BM cells (Ly5.1). Mice were used for BrdU-uptake analysis 12 months after transplantation. BM or spleen $Ly5.1^{+}CD34^{-}KSL$ cells from reconstituted mice were analyzed. (**C**) Lethally irradiated mice (Ly5.2) were transplanted with 3×10^7 spleen cells (Ly5.1). Mice were used for BrdU-uptake analysis 12 months after transplantation. BM or spleen $Ly5.1^{+}CD34^{-}KSL$ cells from reconstituted mice were analyzed.

Published December 6, 2010

JEM

Brief Definitive Report

Therapy-induced selective loss of leukemia-initiating activity in murine adult T cell leukemia

Hiba El Hajj,[1] Marwan El-Sabban,[2] Hideki Hasegawa,[4,5] Ghazi Zaatari,[3] Julien Ablain,[6] Shahrazad T. Saab,[3] Anne Janin,[7] Rami Mahfouz,[3] Rihab Nasr,[1] Youmna Kfoury,[1] Christophe Nicot,[8,9,10] Olivier Hermine,[11] William Hall,[5] Hugues de Thé,[6] and Ali Bazarbachi[1]

[1]Department of Internal Medicine, [2]Department of Human Morphology, and [3]Department of Pathology and Laboratory Medicine, Faculty of Medicine, American University of Beirut, Beirut 1107 2020, Lebanon
[4]Department of Pathology, National Institute of Infectious Diseases, Shinjuku-ku, Tokyo 162 8640, Japan
[5]Centre for Research in Infectious Diseases, School of Medicine and Medical Science, University College Dublin, Dublin 4, Ireland
[6]Service de Biochimie, Equipe labellisée, Ligue Nationale Contre le Cancer, Centre National de la Recherche Scientifique/Institut National de la Santé et de la Recherche Médicale/Université Paris Diderot Unité Mixte de Recherche 7212, Unité 944 and [7]Service de Pathologie, Institut National de la Santé et de la Recherche Médicale/Université Paris Diderot Unité 728, Assistance Publique-Hôpitaux de Paris, Hôpital Saint Louis, 75475 Paris, Cedex 10, France
[8]Department of Pathology and Laboratory Medicine, [9]University of Kansas Cancer Center, and [10]Center for Viral Oncology, University of Kansas Medical Center, Kansas City, KS 66160
[11]Service d'hématologie, Equipe labellisée, Ligue Nationale Contre le Cancer, Centre National de la Recherche Scientifique/Université Paris Descartes Unité Mixte de Recherche 8147, Hôpital Necker-Enfants Malades, 75015 Paris, Cedex 15, France

Chronic HTLV-I (human T cell lymphotropic virus type I) infection may cause adult T cell leukemia/lymphoma (ATL), a disease with dismal long-term prognosis. The HTLV-I transactivator, Tax, initiates ATL in transgenic mice. In this study, we demonstrate that an As_2O_3 and IFN-α combination, known to trigger Tax proteolysis, cures Tax-driven ATL in mice. Unexpectedly, this combination therapy abrogated initial leukemia engraftment into secondary recipients, whereas the primary tumor bulk still grew in the primary hosts, only to ultimately abate later on. This loss of initial transplantability required proteasome function. A similar regimen recently yielded unprecedented disease control in human ATL. Our demonstration that this drug combination targeting Tax stability abrogates tumor cell immortality but not short-term growth may foretell a favorable long-term efficiency of this regimen in patients.

CORRESPONDENCE
Ali Bazarbachi:
bazarbac@aub.edu.lb
OR
Hugues de Thé:
dethe@univ-paris-diderot.fr

Abbreviations used: APL, acute promyelocytic leukemia; ATL, adult T cell leukemia/lymphoma; LIC, leukemia-initiating cell; PLZF, promyelocytic leukemia zinc finger protein; RARA, retinoic acid receptor α; TUNEL, terminal deoxynucleotidyl transferase–mediated nick end labeling.

Adult T cell leukemia/lymphoma (ATL) is one of the rare human cancers initiated by a transforming retrovirus (Matsuoka and Jeang, 2007). The viral transactivator protein Tax was proposed to be an oncogene in ATL, but the fact that Tax protein expression is undetectable in circulating ATL cells has led to significant controversies (Asquith et al., 2000). However, Tax expression in T cells of transgenic mice or in human $CD34^+$ stem cells induces leukemias with striking ATL-like features, including constitutive NF-κB activation, formally demonstrating that Tax initiates ATL (Portis et al., 2001; Hasegawa et al., 2006; Banerjee et al., 2010). Whether continuous Tax expression is required for maintenance of the transformed phenotype is not known. Antiretroviral agents such as zidovudine and IFN-α have shown some efficacy in ATL patients (Gill et al., 1995; Hermine et al., 1995), with complete clinical and hematological responses, although maintenance therapy is required to avoid relapses. Thus, even though the disease may be controlled, it is not cured by this combination. Indeed, human ATL still carries a dismal long-term prognosis (Bazarbachi et al., 2004). Ex vivo, in HTLV-I (human T cell lymphotropic virus type I)–infected human ATL

© 2010 El Hajj et al. This article is distributed under the terms of an Attribution–Noncommercial–Share Alike–No Mirror Sites license for the first six months after the publication date (see http://www.rupress.org/terms). After six months it is available under a Creative Commons License (Attribution–Noncommercial–Share Alike 3.0 Unported license, as described at http://creativecommons.org/licenses/by-nc-sa/3.0/).

The Rockefeller University Press $30.00
J. Exp. Med. Vol. 207 No. 13 2785-2792
www.jem.org/cgi/doi/10.1084/jem.20101095

Supplemental Material can be found at:
http://jem.rupress.org/content/suppl/2010/12/06/jem.20101095.DC1.html

The Journal of Experimental Medicine

Downloaded from jem.rupress.org on May 18, 2011

Published December 6, 2010

cell-lines, As_2O_3 shuts off constitutive NF-κB activation and potentiates the apoptotic effects of IFN-α, at least in part through Tax proteasomal degradation (Bazarbachi et al., 1999; El-Sabban et al., 2000; Nasr et al., 2003). Very recently, a regimen combining As_2O_3, IFN-α, and zidovudine has resulted in unprecedented disease control in de novo patients with the chronic form of the disease (Kchour et al., 2009). Importantly, this regimen does not induce rapid tumor regression and massive cell death, questioning the cellular mechanisms involved. Leukemia-initiating cells (LICs; Dick, 2008) have the unique property to allow full leukemia development and to self-renew. These rare cells may be quantified by limiting dilutions in secondary transplants, and their therapeutic targeting remains a challenge. Yet, in some mouse or human tumor models, most cells appear to have tumor-initiating activity, questioning the hierarchical model established in myeloid leukemias (Kelly et al., 2007; Quintana et al., 2008). In acute promyelocytic leukemia (APL), degradation of the PML/retinoic acid receptor α (RARA) oncogene by the combined effect of retinoic acid and As_2O_3 induces very rapid LIC clearance and definitive cures (Nasr et al., 2008; Hu et al., 2009; Kogan, 2009). Yet, this model is complicated by the fact that differentiation concomitantly clears the tumor bulk. Rapid treatment-induced clearance of tumor-initiating activity that does not initially affect the tumor bulk has never been reported. We performed preclinical experiments in a murine transplantation model of ATL that demonstrate that an IFN-α/As_2O_3 combination abrogates immortal growth and triggers delayed apoptosis, resulting in the cure of ATL recipients. Paradoxically, this drug combination only marginally affects short-term cell proliferation or survival. These results provide a biological basis accounting for the clinical success of IFN-α/As_2O_3/zidovudine therapy in ATL patients.

RESULTS AND DISCUSSION

To explore the in vivo efficacy of IFN-α/As_2O_3, we established ATL transplantation models in which 10^6 ATL spleen cells from one of three independent *Tax* transgenic mice (Hasegawa et al., 2006) were inoculated into SCID mice. All recipients rapidly developed massive hyperleukocytosis, splenomegaly, hypercalcemia, and multiple organ invasion, identical to what is observed in transgenics, and they died within 1 mo (unpublished data). These ATL could be serially passaged for years, with very constant time to death in all recipients, pointing to the remarkable stability of this murine ATL model. We first questioned whether murine ATL cells responded ex vivo to the IFN-α/As_2O_3 combination in the same manner as human ATL cell lines, in which this combination degrades Tax (Fig. 1 A; Bazarbachi et al., 1999; El-Sabban et al., 2000; Nasr et al., 2003). IFN-α or As_2O_3 triggered apoptosis in <20% *Tax* transgenic cells. Their combination killed >80% of cells after ex vivo overnight exposure, whereas normal murine lymphocytes were marginally affected (Fig. S1 A). Tax degradation by the proteasome could not be demonstrated in these ATL cells because the baseline level of protein was undetectable by Western blot analysis (Fig. S1 B; Hasegawa et al., 2006), exactly as in primary human ATLs (Matsuoka and Jeang, 2007). Indeed, *Tax* messenger RNA levels were very similar in primary mouse and human ATL cells, but 1,000-fold higher in HuT-102 cells, in which Tax protein was easily detected (Fig. 1 A and Fig. S1 B).

Mice with well-established leukemias, which had been inoculated 18 d earlier with ATL cells derived from any one of the three independent transgenic founders, were then treated for 3 d with IFN-α, As_2O_3, or both (Fig. 1). Such short IFN-α/As_2O_3 treatment induced a sharp decrease in the number of circulating ATL cells, which, interestingly, was no longer noted when a proteasome inhibitor (PS-341) was concomitantly administered (Fig. 1 B and Fig. S1 C). In contrast, the treatment only marginally affected the spleen weight (Fig. S1 D) and modestly increased baseline apoptosis levels (see Fig. 3 B). Yet, complete reversal of NF-κB activation was observed in ATL spleen cells (Fig. 1 C), as previously observed in human ATL cell lines (El-Sabban et al., 2000), whereas calcium plasma levels returned to normal (Fig. 1 D). Even 6-d IFN-α/As_2O_3 treatment did not significantly decrease the spleen weight (Fig. 1 E and Fig. S1 E). Thus, in contrast to the ex vivo setting, murine ATLs kept on growing under treatment and did not undergo massive and immediate apoptosis.

To investigate any survival benefit, mice were treated earlier, from day 6 to 30 after inoculation of ATL cells. A limited advantage was seen in mice receiving IFN-α or As_2O_3 alone, but a cure (>500-d survival) was noted only among those receiving IFN-α/As_2O_3, and this occurred more frequently when a second course of therapy was administered (T1 + T2; Fig. 1 F). Protocols in which mice were treated only for 5 d per wk never resulted in a cure (unpublished data), pointing to the importance of continuous drug exposure. To follow the fate of ATL cells in the course of this curative therapy, we sacrificed mice at different time points after treatment initiation (Fig. 2 A). Again, at all time points, treatment only moderately affected the spleen weight (Fig. 2 B) but always resulted in diminished circulating ATL cells (not depicted). Pathology examination demonstrated persistent tissue invasion and proliferation even at day 26. Although the frequency of mitoses in leukemic infiltrates of the spleen and liver decreased (Fig. 2, C and D; and Fig. S2 A), Ki-67 expression was maintained. Even though IFN-α/As_2O_3 treatment did not clear the disease, it nevertheless significantly reduced micrometastases within sinusoids of the liver parenchyma (Fig. S2 B). At day 30, when treatment was discontinued, half of the examined mice showed residual actively proliferating leukemic cell invasion, whereas the others exhibited large zones of necrosis with only a few remaining tumor cells and regrowth of normal tissue (not depicted), likely distinguishing cured mice from those that would ultimately die (Fig. 1 F). Importantly, blood cell counts remained highly abnormal when IFN-α/As_2O_3 therapy was discontinued in ultimately cured mice, even in those with rare remaining tumor cells in histological sections (Fig. S2 C). However, at day 180, surviving animals were indistinguishable from noninoculated controls (unpublished data). NF-κB shutoff would be expected to sensitize cells to

Downloaded from jem.rupress.org on May 18, 2011

Published December 6, 2010

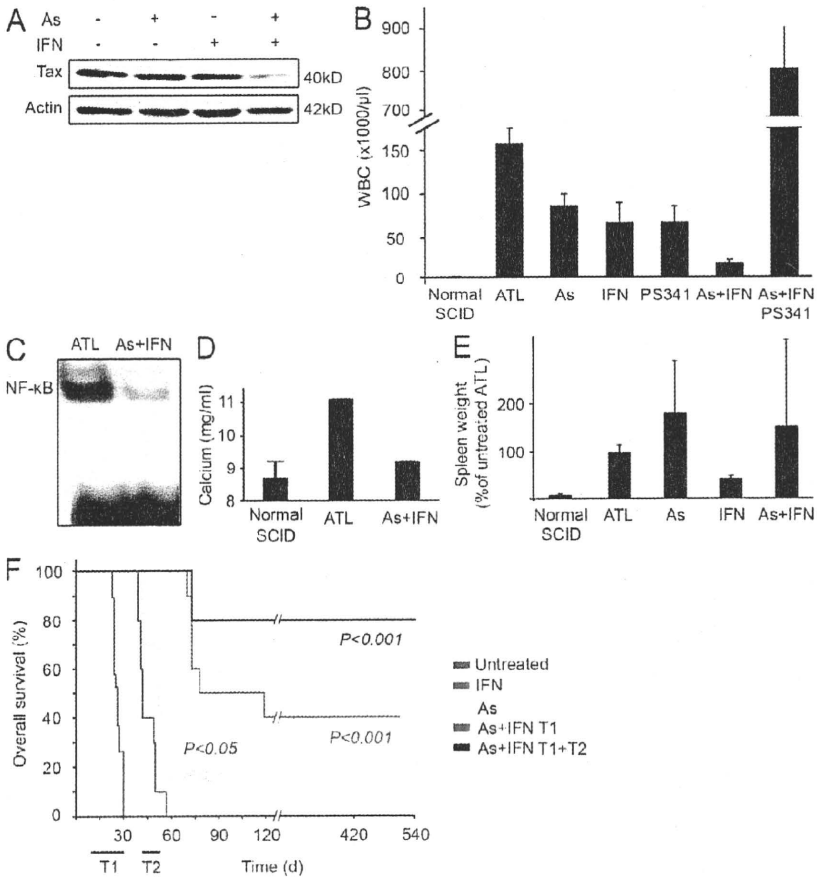

Figure 1. A treatment combining IFN-α and As_2O_3 can cure murine ATL. (A) Western blot analysis of Tax and actin protein expression in human ATL-derived HuT-102 cells after 48 h treatment with As_2O_3 (As), IFN-α, or a combination thereof. (B–D) Effect, at day 18 after inoculation of SCID mice with Tax transgenic splenocytes, of 3-d IFN-α + As_2O_3 treatment on circulating leukemia cell numbers ($n = 3$ for each condition; B). Normal SCID mice were not injected with Tax transgenic splenocytes. NF-κB activation (C) and calcemia ($n = 4$; D) are shown. ATL denotes untreated animals, and PS-341 denotes the proteasome inhibitor. (E) Effect, at day 12 after inoculation of SCID mice with Tax transgenic splenocytes, of 6-d IFN-α + As_2O_3 treatment on spleen weight ($n = 3$). Normal SCID mice were not injected with Tax transgenic splenocytes. (B, D, and E) Error bars show mean ± SD. (F) Kaplan–Meier analysis of overall survival curves of the murine ATL transplant recipients ($n = 10$ for each condition). P-values are indicated. T1 denotes treatment from day 6 to 30; T2 indicates additional treatment from day 42 to 54. This experiment was reproduced three times with similar results.

apoptosis (Portis et al., 2001). Some terminal deoxynucleotidyl transferase–mediated nick end labeling (TUNEL) labeling was noted at days 21 and 26 in vivo (Fig. 2 D and Fig. S2 A) but was massively increased at day 26 ex vivo (Fig. 2 E). Note that TUNEL positivity was always more pronounced in ex vivo than in in vivo labeled cells, possibly because lack of cell to cell contacts precipitates apoptosis. Thus, IFN-α/As_2O_3 elicits delayed apoptosis, which is most likely responsible for the ultimate ATL eradication. Collectively, the IFN-α/As_2O_3 combination cures Tax-driven ATLs, but the tumor grows for weeks under therapy, and it is fully cleared only after treatment discontinuation.

Such a paradoxical pattern of response to therapy in an immunodeficient animal clearly sets this combination aside from most classical cytotoxic anticancer regimens. Thus, we performed serial transplantation experiments in which similar amounts of leukemic spleen cell inoculates from mice untreated or treated for only 3 d with IFN-α and/or As_2O_3 were injected into secondary recipients, which were not subsequently treated (Fig. 3 A). Even when derived from IFN-α/As_2O_3-treated mice, cells used for inoculations were all Tax positive (Fig. S3 A) and were still cycling (Fig. S3 B), and their ex vivo TUNEL labeling was only very modestly increased (Fig. 3 B and Fig. S3 D). Yet, survival of secondary recipients inoculated with ATL cells from IFN-α/As_2O_3-treated primary recipients was dramatically increased with the three independent murine ATLs examined (Fig. 3 C and Fig. S3 C). Comparing the survival of secondary recipients of limiting-dilution inoculates from treated or untreated mice established that IFN-α/As_2O_3 dramatically decreased the ability of ATL cells to initiate leukemia (Fig. 3 D). Indeed, between 1 and 3 ATL cells from untreated donors allowed ATL development, whereas around 1,000 were required when donors had received IFN-α/As_2O_3. Critically, no ATL ever developed in 10 tertiary recipients inoculated with ATL cells from secondary mice inoculated with cells from IFN-α/As_2O_3-treated primary recipients (Fig. 3 E and not depicted).

When moribund secondary recipients were sacrificed, tumor loads (as determined by spleen weight) were slightly decreased in those that had received inoculates from IFN-α/As_2O_3-treated primary recipients (unpublished data). Critically, massive apoptosis was constantly noted in all six untreated leukemic secondary recipients of ATL cells from three independent IFN-α/As_2O_3-treated primary recipients but not in any of the six secondary recipients from untreated donors (Fig. 3 B). Cells derived from infiltrated spleen of these secondary recipients were bona fide ATL cells, as assessed by the fact that they all carried the *Tax* transgene (Fig. S3 F) and had typical morphology (Fig. S3 G and not depicted).

Downloaded from jem.rupress.org on May 18, 2011

Published December 6, 2010

Of note, when proteasome activity was inhibited by PS-341 during the primary recipients' 3-d IFN-α/As_2O_3 therapy, enhanced survival of secondary recipients was curtailed (Fig. 3 C and Fig. S3 C). PS-341 also reversed IFN-α/As_2O_3-induced enhanced apoptosis of ATL cells in the three secondary recipients tested (Fig. 3 B). Finally, all 10 tertiary mice inoculated with ATL cells derived from PS-341/IFN-α/As_2O_3-treated primary donors rapidly died of ATL (Fig. 3 E), in contrast to those with active proteasome. Collectively, a brief exposure to IFN-α/As_2O_3 elicits proteasome-mediated and reversible inheritable cellular changes that preclude long-term tumor propagation but does not affect short-term survival or growth. These cellular changes ultimately result in delayed apoptosis and ATL exhaustion. Such a heritable change could reflect genetic alterations, epigenetic modifications, or some other causes that are yet to be investigated.

As control, we evaluated the effect of the IFN-α/As_2O_3 combination in other leukemias. We found that, in secondary transplant experiments identical to the ones previously performed with ATL cells, PML/RARA-, promyelocytic leukemia zinc finger protein (PLZF)/RARA- or MLL/ENL-transformed cells were marginally (PML/RARA) or not (PLZF/RARA and MLL/ENL) affected by this treatment (Fig. 3 F). This demonstrates that the IFN-α/As_2O_3 combination does not have a general deleterious activity on LIC self-renewal outside of the context of ATL.

That IFN-α/As_2O_3 targets immortal growth in Tax-driven murine ATLs could augur a favorable long-term outcome for As_2O_3/IFN-α/zidovudine-treated chronic ATL patients (Kchour et al., 2009). In that sense, although these patients received a suboptimal 5-d-per-wk treatment, three out of six are still in continuous complete remission 7–18 mo after

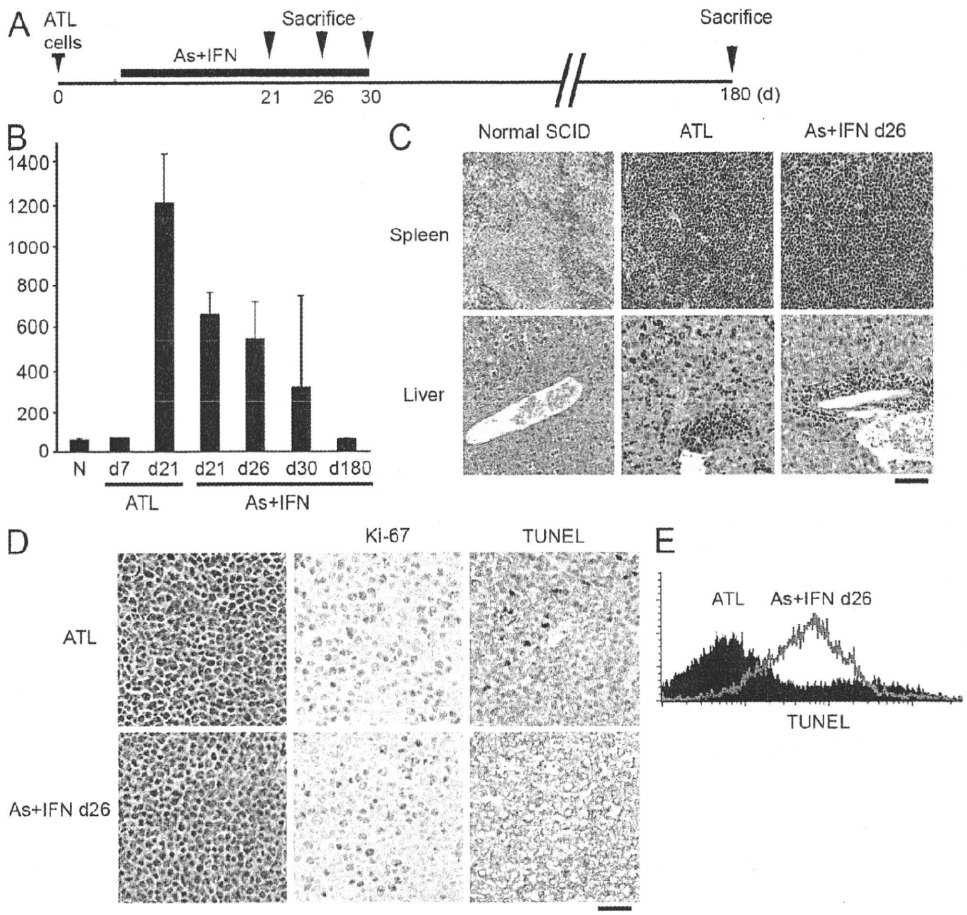

Figure 2. The IFN-α + As_2O_3 combination elicits a moderate decrease of organ infiltration. (A) Experimental design: mice were treated from day 6 up to day 30 after inoculation of ATL cells and sacrificed at different time points after treatment initiation. (B) Spleen weight at various time points during treatment (N: $n = 3$; ATL: d7, $n = 1$; and d21, $n = 5$; and IFN-α + As_2O_3 [As]: d21, $n = 8$; d26, $n = 6$; d30, $n = 6$; and d180, $n = 2$). Error bars show mean ± SD. (C) Histological analysis of the spleen and liver of untreated recipients or at day 26 of IFN-α + As_2O_3 therapy. (D) Ki-67 and TUNEL labeling of spleen leukemia cell infiltrates of untreated recipients or at day 26 of IFN-α + As_2O_3 therapy. (E) TUNEL analysis of ATL cells infiltrating the spleen in untreated recipients or after 26 d of IFN-α + As_2O_3 therapy. Bars: (C) 150 µm; (D) 50 µm.

Downloaded from jem.rupress.org on May 18, 2011

Published December 6, 2010

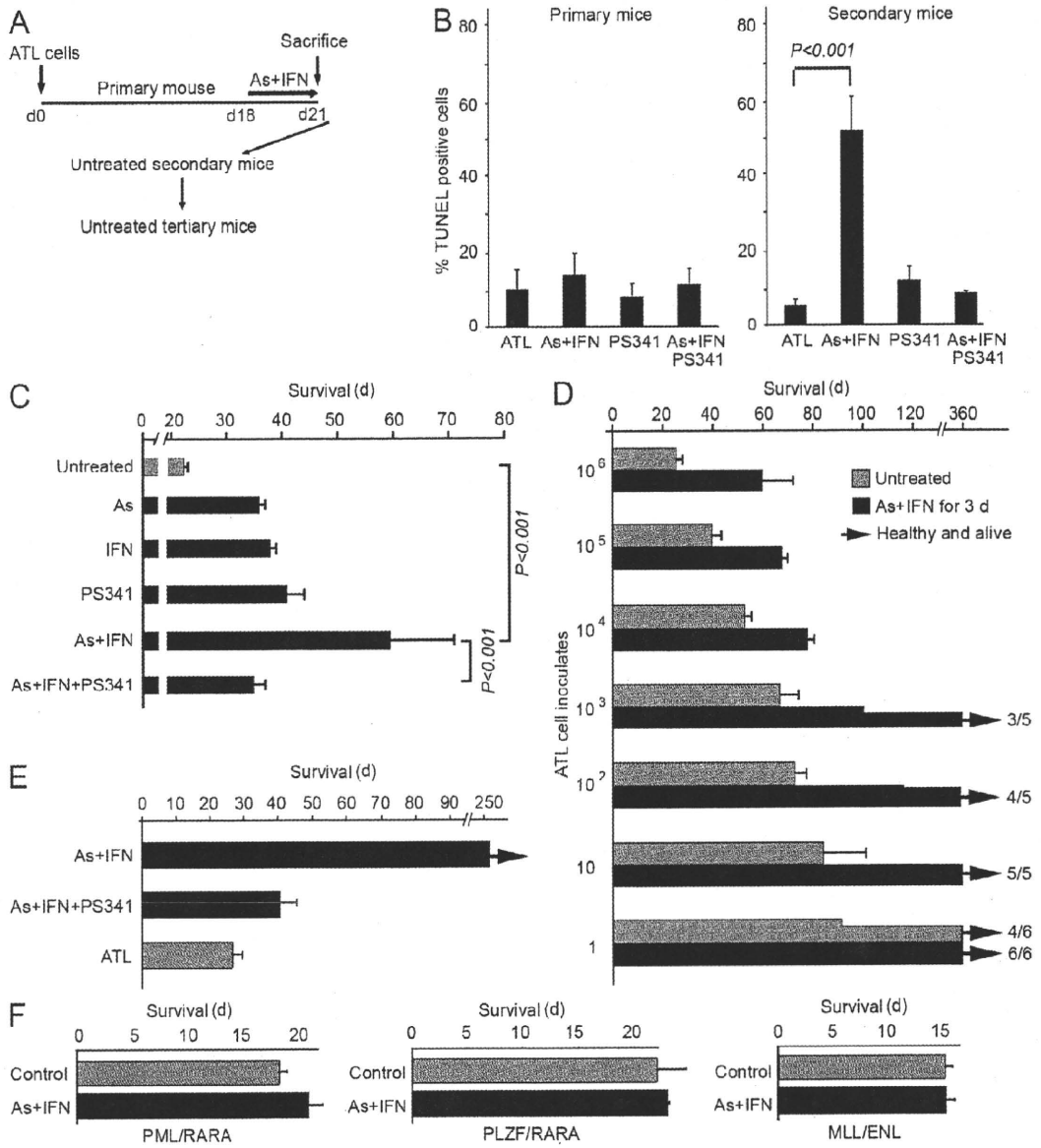

Figure 3. Loss of leukemia-initiating activity accounts for the therapeutic effect of the IFN-α + As_2O_3 combination. (A) Experimental design: serial transplantation of splenocytes from primary mice left untreated or after 3-d IFN-α + As_2O_3 treatment into secondary and tertiary recipients, which were not subsequently treated. (B) TUNEL staining of splenocytes from primary mice left untreated (ATL) or after 3-d IFN-α + As_2O_3 treatment (left) and of splenocytes from secondary recipients of ATL cells from untreated (ATL) or treated primary mice ($n = 6$ for control or IFN-α + As_2O_3 [As]; $n = 3$ for PS-341 or IFN-α + As_2O_3 + PS-341); the p-value is indicated. Secondary recipient cells were analyzed at the time of death of the mice. Secondary mice were not treated. (C) Effect of indicated 3-d treatment of primary donor mice on the survival of secondary recipients of 10^6 spleen ATL cells ($n = 9$ for each condition). This experiment was reproduced twice with similar results, as well as with two other independent primary ATLs (Fig. S3 C). (D) Survival of secondary recipient mice inoculated with varying initial amounts of ATL cells from primary mice either untreated or treated with IFN-α + As_2O_3 for 3 d ($n = 10$ for each condition). (E) Effect of 3-d treatment of primary mice on the survival of tertiary transplants ($n = 10$ for each condition). Secondary recipients were inoculated with 10^6 spleen ATL cells from primary mice. Tertiary recipients were inoculated with 10^6 spleen ATL cells from untreated secondary recipients. Tertiary mice were not treated. (F) Effect of 3-d treatment of primary mice on the survival of secondary recipients of leukemic cells from PML/RARA, PLZF/RARA APLs, or MLL/ENL leukemia ($n = 3$ for each condition). (B–F) Error bars show mean ± SD.

Downloaded from jem.rupress.org on May 18, 2011

Published December 6, 2010

discontinuing maintenance therapy, whereas five ATL patients previously treated with IFN-α/zidovudine alone all relapsed, on average, in less than 5 mo after treatment discontinuation (Table S1). Similarly, in an ongoing trial of ATL lymphoma patients, all six assessable patients are still in complete remission with 3–84-mo follow up after As_2O_3/IFN-α consolidation therapy after initial chemotherapy, which is a distinctly uncommon finding (unpublished data). Although preliminary, these observations suggest nonetheless that in patients, As_2O_3/IFN-α also efficiently targets ATL immortal growth.

To our knowledge, the data presented in this study are the first to decipher the uncoupling between treatment-induced loss of transplantability and continued proliferation of the tumor bulk, which ultimately results in leukemia eradication. *Tax*-driven murine ATL resembles Myc-driven lymphomas or human melanomas, as most cells can initiate tumor formation (Kelly et al., 2007; Quintana et al., 2008). This suggests that the IFN-α/As_2O_3 combination initiates irreversible changes that preclude immortal growth but not short-term proliferation. These changes may restore unidentified checkpoints (such as P53), possibly through epigenetic modifications. Such checkpoint activation triggers delayed apoptosis, as shown both by time course analysis (Fig. 2 E) and transplantation experiments (Fig. 3, C and D). That this delayed apoptosis is fully proteasome dependent strongly suggests the contribution of Tax degradation in the process, hence the specificity of IFN-α/As_2O_3 for ATL cells ex vivo (Bazarbachi et al., 1999; El-Sabban et al., 2000; Nasr et al., 2003) or in vivo (Fig. 3 F). Unfortunately, technical issues of sensitivity preclude the formal demonstration of Tax degradation in vivo and thus definitive conclusion as to the mechanism involved in the effect of therapy. Nevertheless, our data point to the possibility that, in the same manner as in the APL model (Nasr et al., 2008), self-renewal and immortalization require the continuous expression of the driving oncogene, which endows tumor cells with stem cell features (Downing, 2003; Faber and Armstrong, 2007), and the inactivation of which by therapy-induced protein degradation may be a generally applicable strategy.

PML is an IFN-α–induced protein (Stadler et al., 1995) targeted to PML nuclear bodies in an As_2O_3-dependent manner (Zhu et al., 1997). PML was implicated in normal or leukemia stem cell self-renewal (Ito et al., 2008). Through PML degradation, As_2O_3 may thus directly affect LIC self-renewal (Ito et al., 2008). Yet, although As_2O_3 did reduce ATL ability to transplant (Fig. 3 C), it never cleared the disease (Fig. 1 F), possibly because of insufficient exposure. The IFN-α/As_2O_3 combination sequesters PML partner proteins, including Tax, within PML nuclear bodies (Lallemand-Breitenbach et al., 2001, 2008; unpublished data). Like PML, Tax is both sumoylated and ubiquitinated (Nasr et al., 2006; Lallemand-Breitenbach et al., 2008) and might thus be degraded by a PML-dependent mechanism. In addition, IFN-α forces stem cells into the cell cycle (Essers et al., 2009), possibly rendering them more susceptible to As_2O_3.

Treatment of multi-relapsed, IFN-α–resistant, ATL patients with an IFN-α/As_2O_3 regimen has shown some clinical efficacy (Hermine et al., 2004; Ishitsuka et al., 2007). Our latest trial, in which de novo ATL patients were treated with an As_2O_3/IFN-α/zidovudine combination, using suboptimal 5-d-per-wk As_2O_3 administration, has nevertheless yielded unprecedented results (Kchour et al., 2009). Interestingly, in these patients, the kinetics of disease clearance were significantly slower than tumor debulking with cytotoxic drugs. Only partial responses were observed on day 30, and complete remissions slowly unfurled over the next month, whereas three of six patients have remained off treatment for months and are still disease free. These clinical observations are fully in line with the delayed apoptosis observed in ATL mice. That IFN-α/As_2O_3 abrogates immortal growth in Tax-driven murine ATLs, together with the favorable current evolution of many As_2O_3/IFN-α/zidovudine-treated ATL patients, raises the prospect of a possible cure of ATL.

MATERIALS AND METHODS

Mice. We used the ATL mouse model of Hasegawa et al. (2006). To test the effect of different targeted therapies, we established a rapid and reproducible model of disease by direct intraperitoneal transfer of 10^6 spleen cells from Tax transgenic mice into SCID mice (Charles River). Tax expression was detectable only at very low levels by quantitative PCR. PML/RARA and PLZF/RARA APLs were described previously and propagated exactly as before (Nasr et al., 2008). MLL/ENL leukemias were derived from retrovirus infection of primary progenitors from 5-fluorouracyl–treated mice (Lavau et al., 2000). All murine protocols were approved by the Institutional Animal Care and Utilization Committee of the American University of Beirut and the Institut Universitaire d'Hématologie (Université Paris Diderot). All animals were housed in specific pathogen-free facilities. Animals were sacrificed by cervical dislocation after deep anesthesia with isoflurane.

Treatments. As_2O_3 was obtained from Sigma-Aldrich, and recombinant human IFN-α (Roferon) was obtained from Roche. The proteasome inhibitor PS-341 or bortezomib (Velcade) was purchased from Millennium Pharmaceuticals. For in vivo experiments, mice received As_2O_3 (5 μg/g/d) intraperitoneally, IFN-α (10^6 IU/d) subcutaneously, and bortezomib (0.5 mg/kg/d) through mini-osmotic pumps (Alzet; Charles River). These doses are comparable with those used in other mouse models and predicted to yield plasma concentrations similar to those noted in patients (Lallemand-Breitenbach et al., 2008; Nasr et al., 2008; Kogan, 2009). None of the individual or combination treatment regimens were toxic in normal SCID mice (100% survival for >3 mo; $n = 3$ for each condition). In ex vivo experiments, malignant cells from Tax transgenic mice were treated in vitro with 1 μM As_2O_3, 1,000 IU IFN-α, or a combination of both for up to 48 h. Note that the regimen used in ATL mice did not comprise zidovudine because Tax is under the control of the Lck promoter, rather than being expressed from the retrovirus. Treatment protocols for patients with ATL were approved by the ethical committee of Mashhad University of Medical Sciences.

Histopathological and laboratory examination. Tissues from either treated or untreated mice were fixed in neutral buffer formalin (Sigma-Aldrich), embedded in paraffin, sectioned, stained with hematoxylin and eosin, and examined by light microscopy. Ki-67 expression was assessed by immunohistochemistry using rat anti–mouse monoclonal antibodies. Peripheral blood smears were prepared using Giemsa staining. WBC counts and serum calcium levels were determined using routine clinical laboratory techniques. The TUNEL assay was performed on deparaffinized 5-μm sections treated with 20 μg ml^{-1} proteinase K for 15 min at room temperature. The number of TUNEL-positive cells was assessed by two pathologists in three different microscopic fields for each organ studied (liver, lung, and spleen) on a microscope (ProvisAX70; Olympus) with wide-field eye-piece number 26.5 at 600 magnification, which provides a field size of 0.244 mm^2. Mitoses were counted with the same methods, and the results were expressed as the mean number of apoptotic cells or of mitoses per field at 600 magnification.

Downloaded from jem.rupress.org on May 18, 2011

Published December 6, 2010

Cell cycle analysis and TUNEL assay on isolated splenocytes. ATL cells infiltrating the spleen were rapidly harvested, filtered, washed twice with cold PBS, fixed in 100% ethanol at −20°C, and kept overnight at −20°C. Subsequently, cells were rinsed with PBS, treated with Tris-HCl buffer, pH 7.4, containing 1% DNase-free RNase A, and stained with propidium iodide (60 mg/ml final). The distribution of cell cycle phases with different DNA contents was determined using a FACScan flow cytometer (BD). In each sample, 10,000 nongated events were acquired. Analysis of cell cycle distribution (including apoptosis) was performed using CellQuest software (BD).

The TUNEL assay was also used to monitor apoptosis of ATL cells infiltrating the spleen. Splenocytes and ATL cells infiltrating the spleen were rapidly collected, filtered, and washed with cold PBS, and the assay was immediately performed according to the manufacturer's (Roche) recommendations. Fluorescein-conjugated deoxy-UTP incorporated in nucleotide polymers was detected and quantified using flow cytometry. Approximately 10,000 cells per sample were acquired and analyzed using CellQuest software.

Quantitative PCR. Spleens were harvested, and real-time PCR or RT-PCR using a LightCycler (Roche) was used to quantitate the absolute Tax DNA content or Tax messenger RNA expression using a LightCycler Fast-Start DNA Master kit or LightCycler RNA Master kit, respectively. We also used the LightCycler software version 4.05 (Roche). Tax primers SK43I (5′-CGGATACCCAGTCTACGTGT-3′) and SK44I (5′-GAGCCGATA-ACGCGTCCATCG-3′) and probes SK4I-FL (5′-CCCTACTGGCCAC-CTGTCCAGAGC-FL-3′) and SK4I-LC (5′-LC Red640-TCAGATC-ACCTGGGACCCCATCPH-3′) were designed in collaboration with TIB-MOLBIOL. We also used circulating leukemia cells from two acute ATL patients after informed consent. For electrophoretic mobility shift assay, nuclear extracts from splenocytes of treated and untreated mice were prepared as described previously (El-Sabban et al., 2000).

Statistical analysis. Survival curves were calculated according to the method of Kaplan–Meier. Overall survival is defined as the time from injection of ATL cells to death from any cause. Mice that were still alive were censored at the time they were last known to be alive. Analyses were performed using SPSS software version 15.0 (SPSS). The p-value was obtained by log-rank statistical analysis.

Online supplemental material. Fig. S1 shows the effect of short therapy with IFN-α and As_2O_3. Fig. S2 shows the effect of prolonged therapy with IFN-α and As_2O_3. Fig. S3 shows that loss of leukemia-initiating activity accounts for the therapeutic effect of the IFN-α + As_2O_3 combination. Table S1 lists the follow up of ATL patients in complete remission after stopping treatment. Online supplemental material is available at http://www.jem.org/cgi/content/full/jem.20101095/DC1.

We thank C. Leboeuf (Hôpital Saint Louis, Paris, France) for pathology analyses. We warmly thank J.C. Gluckman for reviewing the manuscript.

This work was supported by the American University of Beirut Medical Practice Plan, the University Research Board, and the Lebanese National Council for Scientific Research. H. El Hajj and R. Nasr were supported by the Lady Tata Memorial Trust. H. Hasegawa was supported by Grants-in-Aid for Scientific Research from the Japan Society for the Promotion of Science and grants from the Ministry of Health, Labour, and Welfare Japan and the Takeda Science Foundation. C. Nicot was supported by National Cancer Institute grants CA106258 and CA115398.

The authors declare no financial conflict of interest.

Submitted: 1 June 2010
Accepted: 10 November 2010

REFERENCES

Asquith, B., E. Hanon, G.P. Taylor, and C.R. Bangham. 2000. Is human T-cell lymphotropic virus type I really silent? *Philos. Trans. R. Soc. Lond. B Biol. Sci.* 355:1013–1019. doi:10.1098/rstb.2000.0638

Banerjee, P., A. Tripp, M.D. Lairmore, L. Crawford, M. Sieburg, J.C. Ramos, W. Harrington Jr., M.A. Beilke, and G. Feuer. 2010. Adult T-cell leukemia/lymphoma development in HTLV-1-infected humanized SCID mice. *Blood.* 115:2640–2648. doi:10.1182/blood-2009-10-246959

Bazarbachi, A., M.E. El-Sabban, R. Nasr, F. Quignon, C. Awaraji, J. Kersual, L. Dianoux, Y. Zermati, J.H. Haidar, O. Hermine, and H. de Thé. 1999. Arsenic trioxide and interferon-alpha synergize to induce cell cycle arrest and apoptosis in human T-cell lymphotropic virus type I-transformed cells. *Blood.* 93:278–283.

Bazarbachi, A., D. Ghez, Y. Lepelletier, R. Nasr, H. de Thé, M.E. El-Sabban, and O. Hermine. 2004. New therapeutic approaches for adult T-cell leukaemia. *Lancet Oncol.* 5:664–672. doi:10.1016/S1470-2045(04)01608-0

Dick, J.E. 2008. Stem cell concepts renew cancer research. *Blood.* 112:4793–4807. doi:10.1182/blood-2008-08-077941

Downing, J.R. 2003. The core-binding factor leukemias: lessons learned from murine models. *Curr. Opin. Genet. Dev.* 13:48–54. doi:10.1016/S0959-437X(02)00018-7

El-Sabban, M.E., R. Nasr, G. Dbaibo, O. Hermine, N. Abboushi, F. Quignon, J.C. Ameisen, F. Bex, H. de Thé, and A. Bazarbachi. 2000. Arsenic-interferon-alpha-triggered apoptosis in HTLV-I transformed cells is associated with tax down-regulation and reversal of NF-kappa B activation. *Blood.* 96:2849–2855.

Essers, M.A., S. Offner, W.E. Blanco-Bose, Z. Waibler, U. Kalinke, M.A. Duchosal, and A. Trumpp. 2009. IFNalpha activates dormant haematopoietic stem cells in vivo. *Nature.* 458:904–908. doi:10.1038/nature07815

Faber, J., and S.A. Armstrong. 2007. Mixed lineage leukemia translocations and a leukemia stem cell program. *Cancer Res.* 67:8425–8428. doi:10.1158/0008-5472.CAN-07-0972

Gill, P.S., W. Harrington Jr., M.H. Kaplan, R.C. Ribeiro, J.M. Bennett, H.A. Liebman, M. Bernstein-Singer, B.M. Espina, L. Cabral, S. Allen, et al. 1995. Treatment of adult T-cell leukemia-lymphoma with a combination of interferon alfa and zidovudine. *N. Engl. J. Med.* 332:1744–1748. doi:10.1056/NEJM199506293322603

Hasegawa, H., H. Sawa, M.J. Lewis, Y. Orba, N. Sheehy, Y. Yamamoto, T. Ichinohe, Y. Tsunetsugu-Yokota, H. Katano, H. Takahashi, et al. 2006. Thymus-derived leukemia-lymphoma in mice transgenic for the Tax gene of human T-lymphotropic virus type I. *Nat. Med.* 12:466–472. doi:10.1038/nm1389

Hermine, O., D. Bouscary, A. Gessain, P. Turlure, V. Leblond, N. Franck, A. Buzyn-Veil, B. Rio, E. Macintyre, F. Dreyfus, et al. 1995. Brief report: treatment of adult T-cell leukemia-lymphoma with zidovudine and interferon alfa. *N. Engl. J. Med.* 332:1749–1751. doi:10.1056/NEJM199506293322604

Hermine, O., H. Dombret, J. Poupon, B. Arnulf, F. Lefrère, P. Rousselot, G. Damaj, R. Delarue, J.P. Fermand, J.C. Brouet, et al. 2004. Phase II trial of arsenic trioxide and alpha interferon in patients with relapsed/refractory adult T-cell leukemia/lymphoma. *Hematol. J.* 5:130–134. doi:10.1038/sj.thj.6200374

Hu, J., Y.F. Liu, C.F. Wu, F. Xu, Z.X. Shen, Y.M. Zhu, J.M. Li, W. Tang, W.L. Zhao, W. Wu, et al. 2009. Long-term efficacy and safety of all-trans retinoic acid/arsenic trioxide-based therapy in newly diagnosed acute promyelocytic leukemia. *Proc. Natl. Acad. Sci. USA.* 106:3342–3347. doi:10.1073/pnas.0813280106

Ishitsuka, K., J. Suzumiya, M. Aoki, K. Ogata, S. Hara, and K. Tamura. 2007. Therapeutic potential of arsenic trioxide with or without interferon-alpha for relapsed/refractory adult T-cell leukemia/lymphoma. *Haematologica.* 92:719–720. doi:10.3324/haematol.10703

Ito, K., R. Bernardi, A. Morotti, S. Matsuoka, G. Saglio, Y. Ikeda, J. Rosenblatt, D.E. Avigan, J. Teruya-Feldstein, and P.P. Pandolfi. 2008. PML targeting eradicates quiescent leukaemia-initiating cells. *Nature.* 453:1072–1078. doi:10.1038/nature07016

Kchour, G., M. Tarhini, M.M. Kooshyar, H. El Hajj, E. Wattel, M. Mahmoudi, H. Hatoum, H. Rahimi, M. Maleki, H. Rafatpanah, et al. 2009. Phase 2 study of the efficacy and safety of the combination of arsenic trioxide, interferon alpha, and zidovudine in newly diagnosed chronic adult T-cell leukemia/lymphoma (ATL). *Blood.* 113:6528–6532. doi:10.1182/blood-2009-03-211821

Kelly, P.N., A. Dakic, J.M. Adams, S.L. Nutt, and A. Strasser. 2007. Tumor growth need not be driven by rare cancer stem cells. *Science.* 317:337. doi:10.1126/science.1142596

Kogan, S.C. 2009. Curing APL: differentiation or destruction? *Cancer Cell.* 15:7–8. doi:10.1016/j.ccr.2008.12.012

Downloaded from jem.rupress.org on May 18, 2011

Published December 6, 2010

JEM

Lallemand-Breitenbach, V., J. Zhu, F. Puvion, M. Koken, N. Honoré, A. Doubeikovsky, E. Duprez, P.P. Pandolfi, E. Puvion, P. Freemont, and H. de Thé. 2001. Role of promyelocytic leukemia (PML) sumolation in nuclear body formation, 11S proteasome recruitment, and As_2O_3-induced PML or PML/retinoic acid receptor α degradation. *J. Exp. Med.* 193:1361–1371. doi:10.1084/jem.193.12.1361

Lallemand-Breitenbach, V., M. Jeanne, S. Benhenda, R. Nasr, M. Lei, L. Peres, J. Zhou, J. Zhu, B. Raught, and H. de Thé. 2008. Arsenic degrades PML or PML-RARalpha through a SUMO-triggered RNF4/ubiquitin-mediated pathway. *Nat. Cell Biol.* 10:547–555. doi:10.1038/ncb1717

Lavau, C., R.T. Luo, C. Du, and M.J. Thirman. 2000. Retrovirus-mediated gene transfer of MLL-ELL transforms primary myeloid progenitors and causes acute myeloid leukemias in mice. *Proc. Natl. Acad. Sci. USA.* 97:10984–10989. doi:10.1073/pnas.190167297

Matsuoka, M., and K.T. Jeang. 2007. Human T-cell leukaemia virus type 1 (HTLV-1) infectivity and cellular transformation. *Nat. Rev. Cancer.* 7:270–280. doi:10.1038/nrc2111

Nasr, R., A. Rosenwald, M.E. El-Sabban, B. Arnulf, P. Zalloua, Y. Lepelletier, F. Bex, O. Hermine, L. Staudt, H. de Thé, and A. Bazarbachi. 2003. Arsenic/interferon specifically reverses 2 distinct gene networks critical for the survival of HTLV-1-infected leukemic cells. *Blood.* 101:4576–4582. doi:10.1182/blood-2002-09-2986

Nasr, R., E. Chiari, M. El-Sabban, R. Mahieux, Y. Kfoury, M. Abdulhay, V. Yazbeck, O. Hermine, H. de Thé, C. Pique, and A. Bazarbachi. 2006. Tax ubiquitylation and sumoylation control critical cytoplasmic and nuclear steps of NF-kappaB activation. *Blood.* 107:4021–4029. doi:10.1182/blood-2005-09-3572

Nasr, R., M.C. Guillemin, O. Ferhi, H. Soilihi, L. Peres, C. Berthier, P. Rousselot, M. Robledo-Sarmiento, V. Lallemand-Breitenbach, B. Gourmel, et al. 2008. Eradication of acute promyelocytic leukemia-initiating cells through PML-RARA degradation. *Nat. Med.* 14:1333–1342. doi:10.1038/nm.1891

Portis, T., J.C. Harding, and L. Ratner. 2001. The contribution of NF-kappa B activity to spontaneous proliferation and resistance to apoptosis in human T-cell leukemia virus type 1 Tax-induced tumors. *Blood.* 98:1200–1208. doi:10.1182/blood.V98.4.1200

Quintana, E., M. Shackleton, M.S. Sabel, D.R. Fullen, T.M. Johnson, and S.J. Morrison. 2008. Efficient tumour formation by single human melanoma cells. *Nature.* 456:593–598. doi:10.1038/nature07567

Stadler, M., M.K. Chelbi-Alix, M.H.M. Koken, L. Venturini, C. Lee, A. Saïb, F. Quignon, L. Pelicano, M.-C. Guillemin, C. Schindler, and H. de Thé. 1995. Transcriptional induction of the PML growth suppressor gene by interferons is mediated through an ISRE and a GAS element. *Oncogene.* 11:2565–2573.

Zhu, J., M.H.M. Koken, F. Quignon, M.K. Chelbi-Alix, L. Degos, Z.Y. Wang, Z. Chen, and H. de Thé. 1997. Arsenic-induced PML targeting onto nuclear bodies: implications for the treatment of acute promyelocytic leukemia. *Proc. Natl. Acad. Sci. USA.* 94:3978–3983. doi:10.1073/pnas.94.8.3978

Downloaded from jem.rupress.org on May 18, 2011